

Semiempirical formula for electroweak response functions in the two-nucleon emission channel in neutrino-nucleus scattering

V. L. Martínez-Consentino^{✉,*}, J. E. Amaro^{✉,†} and I. Ruiz Simo^{✉,‡}

Departamento de Física Atómica, Molecular y Nuclear and Instituto Carlos I de Física Teórica y Computacional Universidad de Granada, E-18071 Granada, Spain

 (Received 3 September 2021; accepted 2 December 2021; published 27 December 2021)

A semiempirical formula for the inclusive electroweak response functions in the two-nucleon emission channel is proposed. The method consists in expanding each one of the vector-vector, axial-axial, and vector-axial responses as sums of six subresponses. These correspond to separating the meson-exchange currents as the sum of three currents of similar structure and expanding the hadronic tensor as the sum of the separate contributions from each current plus the interferences between them. For each subresponse, we factorize the coupling constants, the electroweak form factors, the phase space, and the delta propagator, for the delta-forward current. The remaining spin-isospin contributions are encoded in coefficients for each value of the momentum transfer, q . The coefficients are fitted to the exact results in the relativistic mean field model of nuclear matter, for each value of q . The dependence on the energy transfer ω is well described by the semiempirical formula. The q -dependency of the coefficients of the subresponses can be parametrized or can be interpolated from the provided tables. The description of the five theoretical responses is quite good. The parameters of the formula, the Fermi momentum, number of particles, relativistic effective mass, vector energy, the electroweak form factors, and the coupling constants, can be modified easily. This semiempirical formula can be applied to the cross section of neutrinos, antineutrinos, and electrons.

DOI: [10.1103/PhysRevD.104.113006](https://doi.org/10.1103/PhysRevD.104.113006)

I. INTRODUCTION

In recent years, the study of quasielastic neutrino scattering by nuclei has received increasing interest from the theoretical and experimental point of view. This is due to recent neutrino accelerator experiments aimed at measuring neutrino-nucleus cross sections. The ultimate goal is to measure the neutrino oscillation parameters accurately, something that requires knowing with precision the cross sections of neutrino scattering with the nuclei of the detectors. Extensive reviews describing the state of the art of the subject, namely, recent advances and open challenges in the field of neutrino-nucleus scattering, can be found in Refs. [1–9].

Experimental measurements of the inclusive charge-changing (CC) quasielastic cross section (ν_μ, μ^-) and ($\bar{\nu}_\mu, \mu^+$), have been carried out in several laboratories, each of which is characterized by a neutrino flux or distribution in a range of energies with different widths around 1 GeV [10–16]. Comparison of these data with the different nuclear models of the reaction revealed the discrepancies between the different approaches, as well as discrepancies with the

experimental data [17–25]. In particular, the importance of including the contributions of multinucleon emission was highlighted. The calculation of two-particles two-holes (2p2h) contribution varies in different models, but all agree on a contribution that can be around 20% of the cross section with one-nucleon emission only.

Neutrino CC cross sections are averages for different incident energies. Therefore, the differences between models are also differences between averages—although theoretically, the double differential cross section is calculated for fixed neutrino energies. To compare with data for fixed energy, the only possibility is to use the electron (e, e') experiments. This allows the neutrino models to be calibrated, taking into account that the electromagnetic current is related to the vector part of the weak current. It is only the axial current that is not fixed by the electrons. Various approaches to the study of quasielastic lepton scattering have been applied. For finite nuclei quantum Monte Carlo methods [26], continuum shell model with random phase approximation (RPA) correlations [27], or spectral function methods [28,29] can be mentioned. For high or intermediate energies, relativistic corrections are important, yet corrections to kinetic energy can be partially included. But the nuclear interaction at the relativistic level requires a special care [30,31]. The relativistic mean field (RMF) is the simplest model available that includes the

*victormc@ugr.es

†amaro@ugr.es

‡ruizsig@ugr.es

interaction in a fully relativistic way in the form of scalar and vector mean potentials [32,33]. Other models use fits to generate, e.g., parametrizations of the transverse enhancement of the transverse response [19,34]. Most of the approaches require approximations that sometimes violate fundamental current conservation requirements. The influence of other factors such as short-range correlations, final-state interaction, exchange currents, pion emission, and resonance excitation contribute to the differences between the various models and to the difficulty of accurately reproducing electron data in the full kinematical range [35].

In this paper, we focus on the inclusive two-nucleon emission (2p2h) channel for neutrino and electron scattering. Because of the nuclear force between correlated nucleons, a high-energy neutrino can induce emission of a pair of nucleons. In the case of (ν_μ, μ^-) reaction, proton-proton (PP) and proton-neutron (PN) pairs can be ejected, while neutron-neutron (NN) and PN pairs can be ejected in the $(\bar{\nu}_\mu, \mu^+)$ reaction. A large part of the 2p2h cross section is produced by interaction with nuclear meson-exchange currents (MECs), where the exchanged bosons W^\pm are absorbed by mesons exchanged between two nucleons. The most important part of the interaction occurs when the boson absorption by the nucleon produces a virtual Δ that decays and communicates its energy to a pair of nucleons.

Several phenomenological models have been proposed to calculate the 2p2h channel in neutrino interactions. Each of these models, based on the Fermi gas, takes its own approximations, and in general they are numerically expensive. A first calculation revealed the importance of 2p2h to reproduce the data of neutrino scattering [17,36], and similar effects were found in a relativistic calculation [37,38] and also in a local Fermi gas with RPA and other many-body corrections [18,39,40]. These models require integration in many dimensions and intensive numerical computation of traces of two-body operators. Although several approaches have been proposed [41,42] that reduce the calculation, in the absence of analytical formulas for the 2p2h responses, it is necessary to elaborate numerical tables or parametrizations of theoretical calculations for their implementation in Monte Carlo simulators [43,44].

In Ref. [45], the impact of 2p2h was investigated in a simple model using an ansatz physically motivated by the phase-space function of two particles in a Fermi gas. The matrix elements of the MECs averaged over the neutrino flux were approximated by a constant that was fitted to the neutrino data. In this work, we explore extensions of this simple model by adding other physical dependencies, motivated by the theoretical structure of the MEC operators, which contain form factors, coupling constants, and propagators of the Δ , as physical dependencies that must be present in the MEC responses. The rest of the more complex dependencies associated with elements of the spin-isospin matrix of Dirac operators are synthesized in constants for each value of the transferred momentum.

These constants are obtained by a fit of a theoretical model but could also be fitted to data if there were a sufficient number of them. The resulting semiempirical (SE) formula for the MEC responses allows us to compute the inclusive 2p2h responses analytically for fixed q , having the parameters tabulated as a function of q , and to interpolate for intermediate values.

The need of an analytical formula for the inclusive 2p2h responses is based on the difficulty of calculating the integral in seven dimensions for the 2p2h responses, which then has to be integrated with the neutrino flux. With a suitable parametrization, the calculation time is reduced. An alternative parametrization was carried out in the relativistic Fermi gas (RFG) model of Ref. [46] for the vector responses, containing Gaussians and polynomials. A similar parametrization was made in Ref. [20] for the axial contributions. In this paper, we follow a different approach, using the RMF model of nuclear matter and a semiempirical parametrization of the 2p2h responses that has the advantage that the dependence on the momentum, q , and energy transfer, ω , has a theoretical basis. This is analogous to the Bethe-Weizsacker semiempirical mass formula of nuclear binding energy [47], where the dependence on A and Z also has a theoretical basis. In particular, we extract the dependence of the responses on the number of particles, the Fermi momentum, and the relativistic effective mass. Furthermore, the dependence is exact on the form factors and the electroweak coupling constants. The formula will contain constants that we will adjust to the exact results. The frozen and modified convolution approximations have been proposed [41,42] that reduce the integrals to one dimension and five dimensions, respectively, to which an integral over the neutrino flux would have to be added. However, the semiempirical formula has the advantage that it is analytical and gives better results than the frozen one, since the parameters have been adjusted to reproduce the exact responses.

Note that the developments in this paper are applicable to the calculation of inclusive cross sections only. The MEC model that we use to fit the SE-MEC responses is based on Feynman diagrams for pion production on the nucleon. In our case, these diagrams will be considered in a RMF model of nuclear matter. In this model, the nucleons are relativistic and interact with vector and scalar potentials, the effect of which is to give them an effective mass and a repulsive vector energy. The idea is to combine this SE-MEC formula with the superscaling approach with relativistic effective mass M^* (SuSAM*) in which a new scaling function $f^*(\psi^*)$ including dynamical relativistic effects has been proposed [48–50] through the introduction of an effective mass for the nucleon. The SuSAM* model describes a large amount of the electron data within a phenomenological quasielastic band, and it was extended to the neutrino and antineutrino sector [51], SuSAM* was first developed from the set of ^{12}C data [48,49] and later

applied to other nuclei in Refs. [50,52]. Recently, the superscaling function has been refitted by subtraction of the MEC 2p2h cross section before performing the scaling analysis, in order to avoid double-counting when adding the MEC responses [53].

The scheme of the paper is as follows. In Sec. II, we present the formalism for neutrino scattering, the inclusive 2p2h hadronic tensor, the model of MEC, the analytical approximation of the phase-space integral in frozen nucleon approximation, and the averaged Δ propagator. In Sec. III, we write the semiempirical formula for the MEC responses. In Sec. IV, we present the results of the fit and compare with the exact results. In Sec. V, we draw our conclusions.

II. FORMALISM OF CC NEUTRINO SCATTERING

A. Neutrino cross section

In this section, we summarize the formalism for charge-changing neutrino scattering. The case of electron scattering can be easily inferred from this by considering only the longitudinal and transverse response functions. Thus, we consider charged-current inclusive quasielastic reactions in nuclei induced by neutrinos and antineutrinos, focusing on the (ν_μ, μ^-) and $(\bar{\nu}_\mu, \mu^+)$ cross sections. The relativistic energies of the incident (anti)neutrino and detected muon are $\epsilon = E_\nu$, and $\epsilon' = m_\mu + T_\mu$, respectively. Their momenta are \mathbf{k} and \mathbf{k}' . The 4-momentum transfer is $k^\mu - k'^\mu = Q^\mu = (\omega, \mathbf{q})$, with $Q^2 = \omega^2 - q^2 < 0$. The lepton scattering angle, θ , is the angle between \mathbf{k} and \mathbf{k}' . The double-differential cross section can be written as

$$\frac{d^2\sigma}{dT_\mu d\cos\theta} = \frac{G^2 \cos^2\theta_c}{4\pi} \frac{k'}{\epsilon} v_0 [V_{CC}R_{CC} + 2V_{CL}R_{CL} + V_{LL}R_{LL} + V_{TR}R_T \pm 2V_{T'}R_{T'}]. \quad (1)$$

Inside the brackets in Eq. (1), there is a linear combination of the five nuclear response functions, where (+) is for neutrinos and (−) is for antineutrinos. Here, $G = 1.166 \times 10^{-11} \text{ MeV}^{-2}$ is the Fermi constant, θ_c is the Cabibbo angle, $\cos\theta_c = 0.975$, and the kinematical factor $v_0 = (\epsilon + \epsilon')^2 - q^2$. The V_K coefficients depend only on the lepton kinematics and do not depend on the details of the nuclear target,

$$V_{CC} = 1 + \delta^2 \frac{Q^2}{v_0} \quad (2)$$

$$V_{CL} = \frac{\omega}{q} - \frac{\delta^2 Q^2}{\rho' v_0} \quad (3)$$

$$V_{LL} = \frac{\omega^2}{q^2} - \left(1 + \frac{2\omega}{q\rho'} + \rho\delta^2\right) \delta^2 \frac{Q^2}{v_0} \quad (4)$$

$$V_T = -\frac{Q^2}{v_0} + \frac{\rho}{2} + \frac{\delta^2}{\rho'} \left(\frac{\omega}{q} + \frac{1}{2}\rho\rho'\delta^2\right) \frac{Q^2}{v_0} \quad (5)$$

$$V_{T'} = -\frac{1}{\rho'} \left(1 - \frac{\omega\rho'}{q}\delta^2\right) \frac{Q^2}{v_0}, \quad (6)$$

where we have defined the dimensionless factors $\delta = m_\mu/\sqrt{|Q^2|}$, proportional to the muon mass m_μ , $\rho = |Q^2|/q^2$, and $\rho' = q/(\epsilon + \epsilon')$.

The response functions, $R^K(q, \omega)$, are defined as suitable combinations of the hadronic tensor, $W^{\mu\nu}$, in a reference frame where the z axis ($\mu = 3$) points along the momentum transfer \mathbf{q} and the x axis ($\mu = 1$) is defined as the transverse (to \mathbf{q}) component of the (anti)neutrino momentum \mathbf{k} lying in the lepton scattering plane; the y axis ($\mu = 2$) is then normal to the lepton scattering plane. The usual components are then

$$R^{CC} = W^{00} \quad (7)$$

$$R^{CL} = -\frac{1}{2}(W^{03} + W^{30}) \quad (8)$$

$$R^{LL} = W^{33} \quad (9)$$

$$R^T = W^{11} + W^{22} \quad (10)$$

$$R^{T'} = -\frac{i}{2}(W^{12} - W^{21}). \quad (11)$$

The inclusive hadronic tensor is constructed from the matrix elements of the current operator $J^\mu(Q)$ between the initial and final hadronic states, summing over all the possible final nuclear states with excitation energy $\omega = E_f - E_i$ and averaging over the initial spin components,

$$W^{\mu\nu} = \sum_f \overline{\sum_i} \langle f | J^\mu(Q) | i \rangle^* \langle f | J^\nu(Q) | i \rangle \delta(E_i + \omega - E_f). \quad (12)$$

In the case of electron scattering, the cross section is

$$\frac{d\sigma}{d\Omega d\epsilon'} = \sigma_{\text{Mott}}(v_L R_{em}^L + v_T R_{em}^T). \quad (13)$$

where σ_{Mott} is the Mott cross section, v_L and v_T are kinematic factors

$$v_L = \frac{Q^4}{q^4} \quad (14)$$

$$v_T = \tan^2\theta - \frac{Q^2}{2q^2}. \quad (15)$$

The electromagnetic longitudinal and transverse response functions, $R_{em}^L(q, \omega)$ and $R_{em}^T(q, \omega)$, are

$$R_{em}^L = W_{em}^{00} \quad (16)$$

$$R_{em}^T = W_{em}^{11} + W_{em}^{22}. \quad (17)$$

Attending to the kind of final states, the hadronic tensors can be written as sum of one-particle (1p1h) plus two-particles (2p2h),..., emission channels

$$W^{\mu\nu} = W_{1p1h}^{\mu\nu} + W_{2p2h}^{\mu\nu} + \dots \quad (18)$$

In this work, we are interested in the 2p2h channel only. We studied the 1p1h responses and cross section for CC neutrino and antineutrino scattering in Ref. [51] and for electron scattering in Refs. [50,52,53]. Here, we extend these works to deepen the study of the interaction of neutrinos with nuclei at intermediate energies and the role of the 2p2h electroweak response functions, as described in the next subsection.

B. 2p2h hadronic tensor in the RMF

In this paper, we consider the 2p2h responses within the RMF model of nuclear matter [54–57]. In this model, the nucleons are interacting with a relativistic field containing scalar and vector potentials. The single-particle wave functions are plane waves with momentum \mathbf{h} and with on-shell energy

$$E = \sqrt{(m_N^*)^2 + h^2}, \quad (19)$$

where m_N^* is the relativistic effective mass of the nucleon defined by

$$m_N^* = m_N - g_s \phi_0 = M^* m_N, \quad (20)$$

where m_N is the bare nucleon mass, $g_s \phi_0$ is the scalar potential energy of the RMF [55], and $M^* = 0.8$ for ^{12}C , the nucleus considered in our results. Additionally, the nucleon acquires a positive energy due to the repulsion by the relativistic vector potential, $E_v = g_v V_0$. Thus, the total nucleon energy is

$$E_{\text{RMF}} = E + E_v. \quad (21)$$

In this work, we use values of k_F , M^* and E_v that are obtained phenomenologically from the data of (e, e') [53]. In particular, we use the value $E_v = 141$ MeV for ^{12}C . In the semiempirical formulas in the next section, these values could easily be modified if desired. For many observables, that only depend on the energy differences between a final particle and an initial one, the vector energy cancels out and does not affect the results.

The nuclear states in the RMF are Slater determinants constructed with plane waves obtained by solving the free Dirac equation with effective mass m_N^* . Note that we use the same effective mass for particles and holes. In this approximation, the model is the simplest possible that implements the mean field, so the results for very large momenta should be taken with caution.

All states with momentum $h < k_F$ are occupied in the ground state, with k_F the Fermi momentum. The 2p2h excitations are obtained by raising two particles above the Fermi level, with momenta p'_1 and $p'_2 > k_F$, leaving two holes with momenta h_1 and $h_2 < k_F$. In this work, we focus on the 2p2h part of the hadronic tensor. It is generated by the interaction with a two-body current operator, whose matrix elements are given by

$$\begin{aligned} \langle f | J^\mu(Q) | i \rangle &= \frac{(2\pi)^3}{V^2} \delta(\mathbf{p}'_1 + \mathbf{p}'_2 - \mathbf{q} - \mathbf{h}_1 - \mathbf{h}_2) \\ &\times \frac{(m_N^*)^2}{\sqrt{E'_1 E'_2 E_1 E_2}} j^\mu(\mathbf{p}'_1, \mathbf{p}'_2, \mathbf{h}_1, \mathbf{h}_2), \end{aligned} \quad (22)$$

where V is the volume of the system and the on-shell energies and momenta of the particles and holes are (E'_i, \mathbf{p}'_i) , and (E_i, \mathbf{h}_i) , for $i = 1, 2$. Note that 3-momentum is conserved and that the relativistic factors $(m_N^*/E)^{1/2}$ contain the effective mass and the on-shell energies. The spin-isospin two-body current matrix elements $j^\mu(\mathbf{p}'_1, \mathbf{p}'_2, \mathbf{h}_1, \mathbf{h}_2)$ are defined in the next subsection.

Inserting this expression into the hadronic tensor, Eq. (12), and taking the limit $V \rightarrow \infty$ (infinite nuclear matter), we transform the sums into integrals, to obtain the 2p2h hadronic tensor for the RMF theory of nuclear matter

$$\begin{aligned} W_{2p2h}^{\mu\nu} &= \frac{V}{(2\pi)^9} \int d^3 p'_1 d^3 p'_2 d^3 h_1 d^3 h_2 \\ &\times \frac{(m_N^*)^4}{E_1 E_2 E'_1 E'_2} w^{\mu\nu}(\mathbf{p}'_1, \mathbf{p}'_2, \mathbf{h}_1, \mathbf{h}_2) \\ &\times \Theta(p'_1, h_1) \Theta(p'_2, h_2) \delta(E'_1 + E'_2 - E_1 - E_2 - \omega) \\ &\times \delta(\mathbf{p}'_1 + \mathbf{p}'_2 - \mathbf{q} - \mathbf{h}_1 - \mathbf{h}_2), \end{aligned} \quad (23)$$

where $V/(2\pi)^3 = Z/(\frac{8}{3}\pi k_F^3)$ for symmetric nuclear matter. The Pauli blocking function Θ is defined as the product of step functions for the initial and final momentum

$$\Theta(p'_i, h_i) \equiv \theta(p'_i - k_F) \theta(k_F - h_i). \quad (24)$$

Finally, the function $w^{\mu\nu}(\mathbf{p}'_1, \mathbf{p}'_2, \mathbf{h}_1, \mathbf{h}_2)$ represents the hadron tensor for a single 2p2h transition, summed up over spin and isospin,

$$w^{\mu\nu}(\mathbf{p}'_1, \mathbf{p}'_2, \mathbf{h}_1, \mathbf{h}_2) = \frac{1}{4} \sum_{s_1 s_2 s'_1 s'_2} \sum_{t_1 t_2 t'_1 t'_2} j^\mu(1', 2', 1, 2)_A^* j^\nu(1', 2', 1, 2)_A. \quad (25)$$

The two-body current matrix elements is antisymmetrized,

$$j^\mu(1', 2', 1, 2)_A \equiv j^\mu(1', 2', 1, 2) - j^\mu(1', 2', 2, 1). \quad (26)$$

The factor 1/4 in Eq. (25) accounts for the antisymmetry of the two-body wave function with respect to exchange of momenta, spin, and isospin quantum numbers.

In this work, we use Eq. (23) to compute the five 2p2h inclusive response functions R_{CC} , R_{CL} , R_{LL} , R_T , $R_{T'}$, for neutrino and antineutrino scattering. Integrating over \mathbf{p}'_2 using the momentum delta function, these responses are given by

$$R_{2p2h}^K = \frac{V}{(2\pi)^9} \int d^3 p'_1 d^3 h_1 d^3 h_2 \frac{(m_N^*)^4}{E_1 E_2 E'_1 E'_2} \Theta(p'_1, h_1) \times \Theta(p'_2, h_2) r^K(\mathbf{p}'_1, \mathbf{p}'_2, \mathbf{h}_1, \mathbf{h}_2) \times \delta(E'_1 + E'_2 - E_1 - E_2 - \omega), \quad (27)$$

where $\mathbf{p}'_2 = \mathbf{h}_1 + \mathbf{h}_2 + \mathbf{q} - \mathbf{p}'_1$. The five elementary response functions for a 2p2h excitation r^K are defined in Eqs. (7)–(11), in terms of the elementary hadronic tensor $w^{\mu\nu}$, Eq. (25), for $K = CC, CL, LL, T, T'$. Because of axial

symmetry around the momentum transfer \mathbf{q} (the z axis), we can fix the azimuthal angle of the first particle, $\phi'_1 = 0$ and multiply by 2π . Finally, the energy delta function allows us to integrate analytically over p'_1 , reducing Eq. (27) to 7-dimensional integral, that we compute numerically [58].

C. Electroweak meson-exchange currents

In this work, we use the electroweak MEC model described by the nine Feynman diagrams depicted in Fig. 1. The two-body current matrix elements $j^\mu(1', 2', 1, 2)$ corresponding to this model enter in the calculation of the elementary 2p2h hadronic tensor, Eq. (25). The different contributions have been taken from the pion weak production model of Ref. [59].

To obtain the MEC, we have started from the pion production currents given in Eq. (51) of Ref. [59], and we have applied the Goldberger-Treiman relation $f_{\pi NN}/m_\pi = g_A/(2f_\pi)$, with $f_\pi = 93$ MeV, to factorize a common coupling constant $f_{\pi NN}/m_\pi$ in all vertices πNN . We have not included the nucleon-pole diagrams where the W^\pm -boson is coupled to the nucleon current, since these diagrams are not considered part of the MEC and are not taken into account here. Some previous calculations of the correlations in the 2p2h channel, of pionic type [60] or of Jastrow type [61], indicate that their effect when added to the one-body response is to produce a tail to the right of the Quasielastic (QE) peak of the order of 10% of the total height.

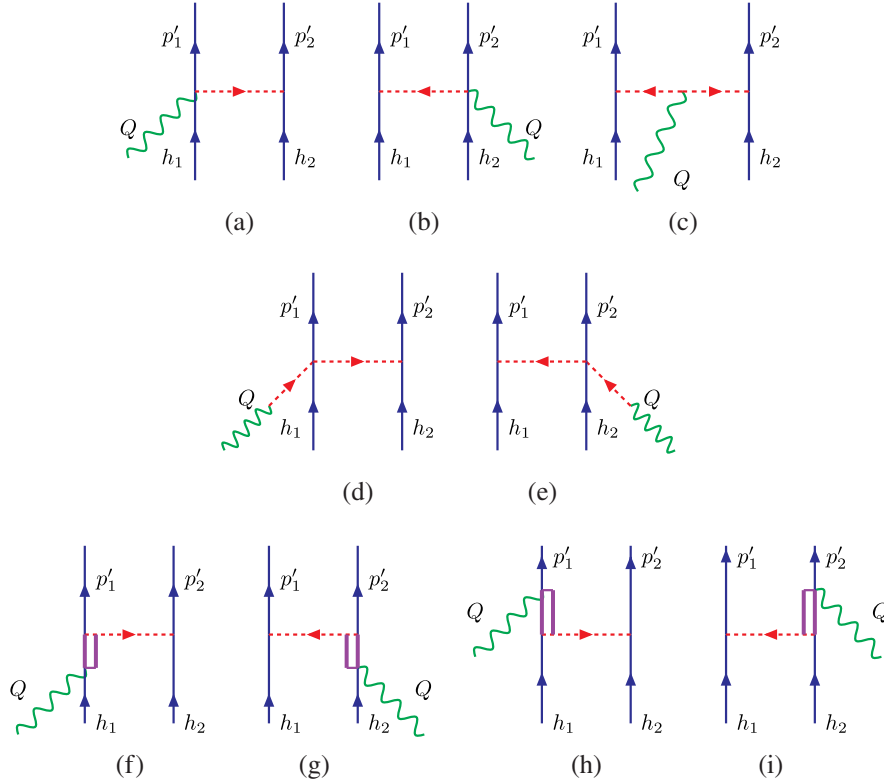


FIG. 1. Feynman diagrams for the electroweak MEC model used in this work.

The MEC is the sum of four two-body currents: seagull (diagrams a and b), pion in flight (diagram c), pion-pole (diagrams d and e), and $\Delta(1232)$ excitation forward (diagrams f and g), and backward (diagrams h and i).

$$j_{\text{sea}}^{\mu} = [I_{\bar{V}}^{\pm}]_{1'2',12} \frac{f_{\pi NN}^2}{m_{\pi}^2} V_{\pi NN}^{s'_1 s_1}(\mathbf{p}'_1, \mathbf{h}_1) F_{\pi NN}(k_1^2) \bar{u}_{s'_2}(\mathbf{p}'_2) \left[F_1^V(Q^2) \gamma_5 \gamma^{\mu} + \frac{F_{\rho}(k_2^2)}{g_A} \gamma^{\mu} \right] u_{s_2}(\mathbf{h}_2) + (1 \leftrightarrow 2) \quad (28)$$

$$j_{\pi}^{\mu} = [I_{\bar{V}}^{\pm}]_{1'2',12} \frac{f_{\pi NN}^2}{m_{\pi}^2} F_1^V(Q^2) V_{\pi NN}^{s'_1 s_1}(\mathbf{p}'_1, \mathbf{h}_1) V_{\pi NN}^{s'_2 s_2}(\mathbf{p}'_2, \mathbf{h}_2) (k_1^{\mu} - k_2^{\mu}) \quad (29)$$

$$j_{\text{pole}}^{\mu} = [I_{\bar{V}}^{\pm}]_{1'2',12} \frac{f_{\pi NN}^2}{m_{\pi}^2} \frac{F_{\rho}(k_1^2)}{g_A} F_{\pi NN}(k_2^2) \frac{Q^{\mu} \bar{u}_{s'_1}(\mathbf{p}'_1) \not{Q} u_{s_1}(\mathbf{h}_1)}{Q^2 - m_{\pi}^2} V_{\pi NN}^{s'_2 s_2}(\mathbf{p}'_2, \mathbf{h}_2) + (1 \leftrightarrow 2) \quad (30)$$

$$j_{\Delta F}^{\mu} = [U_{\bar{F}}^{\pm}]_{1'2',12} \frac{f^* f_{\pi NN}}{m_{\pi}^2} V_{\pi NN}^{s'_2 s_2}(\mathbf{p}'_2, \mathbf{h}_2) F_{\pi N \Delta}(k_2^2) \bar{u}_{s'_1}(\mathbf{p}'_1) k_2^{\alpha} G_{\alpha\beta}(h_1 + Q) \Gamma^{\beta\mu}(Q) u_{s_1}(\mathbf{h}_1) + (1 \leftrightarrow 2). \quad (31)$$

$$j_{\Delta B}^{\mu} = [U_{\bar{B}}^{\pm}]_{1'2',12} \frac{f^* f_{\pi NN}}{m_{\pi}^2} V_{\pi NN}^{s'_2 s_2}(\mathbf{p}'_2, \mathbf{h}_2) F_{\pi N \Delta}(k_2^2) \bar{u}_{s'_1}(\mathbf{p}'_1) k_2^{\beta} \hat{\Gamma}^{\mu\alpha}(Q) G_{\alpha\beta}(p'_1 - Q) u_{s_1}(\mathbf{h}_1) + (1 \leftrightarrow 2). \quad (32)$$

where $k_i^{\mu} = (p'_i - h_i)^{\mu}$ is the 4-momentum transferred to the i th nucleon. Note that the energy of each nucleon includes the vector energy, Eq. (21), but the vector energies of the initial and final nucleons cancel out when computing the components $k_i^0 = E'_i - E_i$.

In these equations, we have defined the following function:

$$V_{\pi NN}^{s'_1 s_1}(\mathbf{p}'_1, \mathbf{h}_1) \equiv F_{\pi NN}(k_1^2) \frac{\bar{u}_{s'_1}(\mathbf{p}'_1) \gamma_5 \not{k}_1 u_{s_1}(\mathbf{h}_1)}{k_1^2 - m_{\pi}^2}. \quad (33)$$

This function appears in all the currents, describing the propagation and emission (or absorption) of the exchanged pion, having a strong form factor $F_{\pi NN}$ given by [62,63]

$$F_{\pi NN}(k_1^2) = \frac{\Lambda^2 - m_{\pi}^2}{\Lambda^2 - k_1^2} \quad (34)$$

and $\Lambda = 1300$ MeV.

The charge dependence of the currents in the different p-n channels is determined by the matrix elements of the isospin operators $I_{\bar{V}}^{\pm}$, $U_{\bar{F}}^{\pm}$, and $U_{\bar{B}}^{\pm}$, where the $+$ ($-$) sign refers to neutrino (antineutrino) scattering. They are defined by

$$I_{\bar{V}}^{\pm} = (I_V)_x \pm i(I_V)_y \quad (35)$$

$$U_{\bar{F}}^{\pm} = (U_F)_x \pm i(U_F)_y \quad (36)$$

$$U_{\bar{B}}^{\pm} = (U_B)_x \pm i(U_B)_y, \quad (37)$$

where

$$I_V = i[\tau(1) \times \tau(2)] \quad (38)$$

$$(U_F)_j = \sqrt{\frac{3}{2}} \sum_{i=1}^3 (T_i T_j^{\dagger}) \otimes \tau_i \quad (39)$$

$$(U_B)_j = \sqrt{\frac{3}{2}} \sum_{i=1}^3 (T_j T_i^{\dagger}) \otimes \tau_i, \quad (40)$$

where \vec{T} is an isovector transition operator from isospin $\frac{3}{2}$ to $\frac{1}{2}$.

Additionally, each current contains coupling constants and electroweak form factors. The coupling constants are $f_{\pi NN} = 1$, $g_A = 1.26$, and $f^* = 2.13$.

The electroweak form factors are $F_1^V = F_1^p - F_1^n$ in the seagull vector and pion-in flight currents, for which we use Galster's parametrization [64], and F_{ρ} in the axial seagull and pion-pole currents, taken from Ref. [59]. In the case of the Δ current, we use the form factors C_3^V and C_5^A , respectively, for the vector and axial parts of the current [59]. These appear in the $N \rightarrow \Delta$ transition vertex in the forward current

$$\Gamma^{\beta\mu}(Q) = \frac{C_3^V}{m_N} (g^{\beta\mu} \not{Q} - Q^{\beta} \gamma^{\mu}) \gamma_5 + C_5^A g^{\beta\mu} \quad (41)$$

and for the backward current

$$\hat{\Gamma}^{\mu\alpha}(Q) = \gamma^0 [\Gamma^{\alpha\mu}(-Q)]^{\dagger} \gamma^0. \quad (42)$$

The vector and axial form factors in the Δ current are from Ref. [59],

$$C_3^V(Q^2) = \frac{2.13}{(1 - Q^2/M_V^2)^2} \frac{1}{1 - \frac{Q^2}{4M_V^2}},$$

$$C_5^A(Q^2) = \frac{1.2}{(1 - Q^2/M_{A\Delta}^2)^2} \frac{1}{1 - \frac{Q^2}{4M_{A\Delta}^2}}, \quad (43)$$

with $M_V = 0.84$ GeV and $M_{A\Delta} = 1.05$ GeV.

We use the $\pi N\Delta$ strong form factor of Ref. [65], given by

$$F_{\pi N\Delta}(k_2^2) = \frac{\Lambda_\Delta^2}{\Lambda_\Delta^2 - k_2^2}, \quad (44)$$

where $\Lambda_\Delta = 1150$ MeV.

Finally, the Δ -propagator, including the decay width of the $\Delta(1232)$, is given by

$$G_{\alpha\beta}(P) = \frac{\mathcal{P}_{\alpha\beta}(P)}{P^2 - M_\Delta^2 + iM_\Delta\Gamma_\Delta(P^2) + \frac{\Gamma_\Delta(P^2)^2}{4}}. \quad (45)$$

The projector $\mathcal{P}_{\alpha\beta}(P)$ over spin- $\frac{3}{2}$ on-shell particles is given by

$$\mathcal{P}_{\alpha\beta}(P) = -(\not{P} + M_\Delta) \times \left[g_{\alpha\beta} - \frac{1}{3}\gamma_\alpha\gamma_\beta - \frac{2P_\alpha P_\beta}{3M_\Delta^2} + \frac{1P_\alpha\gamma_\beta - P_\beta\gamma_\alpha}{3M_\Delta} \right]. \quad (46)$$

This concludes the description of the electroweak current. The spinors of particles and holes are calculated in the RMF model with the relativistic effective mass m_N^* instead of m_N , and with on-shell energy, Eq. (19). The total nucleon energy in the RMF (21) includes the vector energy, E_v . As can be seen, this vector energy cancels out in the terms of the currents that depend on the vectors k_i^μ . But it is not canceled in the delta propagator, which is the only place where E_v will appear explicitly.

Note that when considering the free Δ without self-energy we are neglecting the interaction of the Δ in the medium. The case of the interacting Delta is summarized in Appendix A and is briefly discussed at the end of Sec. IV.

The seagull current has a vector and an axial part. The pionic current is pure vector, and the pion-pole current is pure axial. However, the pion-pole could be considered as the axial part of the pion in flight in a certain sense. The Δ -forward and backward currents have a vector and an axial part also.

In the case of electron scattering, the above formulas are valid, but only the vector part of the current appears. Thus, the pion-pole diagrams (d and e) are not contributing. The isospin operators are modified to the z component instead of the \pm component [53]. Only the L and T responses are present in (e, e')

The exact calculation of the response functions $R_K(q, \omega)$ with this model of currents is carried out by numerical integration in seven dimensions of Eq. (27). The spin sums

are performed numerically. The isospin channels in the case of neutrino CC scattering are pn and pp in the final states. These two channels are computed separately and then added to obtain the total responses. More details on the calculation are given in Ref. [66].

Note that the same 2p2h responses were calculated in a previous work [20,46] with a similar MEC model. The differences with our new model are in the description of the Δ propagator, which is included here in its entirety, while in Refs. [20,46], only the real part of the denominator of the Δ propagator was included. The second difference is that in the present model the nucleon wave functions are solutions of the Dirac equation in the mean field, that is, Dirac plane waves with relativistic effective mass and vector energy. On the contrary, in Refs. [20,46], a RFG without effective mass was used, but including an energy shift of 40 MeV. As seen in Ref. [53], the effect of the imaginary part of the propagator is to increase the contribution of the ΔF diagram and the position of the maximum. The effect of the effective mass and vector energy is to reduce the height of the peak, which partially compensates for the difference of the MEC with respect to the calculation of Refs. [20,46].

Finally, the present model is restricted to a neutrino energy range in which excitations of higher resonances, beyond the Delta, are not essential. This is good enough for experiments like T2K but not for DUNE.

D. Phase-space integral

Part of the dependence of the 2p2h response as a function of q and ω will be associated with the number of 2p2h states that can be excited while conserving energy and momentum. That number is proportional to the phase-space function. In the RMF of nuclear matter, it is given by

$$F(q, \omega) = \int d^3p'_1 d^3h_1 d^3h_2 \frac{(m_N^*)^4}{E_1 E_2 E'_1 E'_2} \Theta(p'_1, h_1) \times \Theta(p'_2, h_2) \delta(E'_1 + E'_2 - E_1 - E_2 - \omega), \quad (47)$$

where $\mathbf{p}'_2 = \mathbf{h}_1 + \mathbf{h}_2 + \mathbf{q} - \mathbf{p}'_1$. This function was fully studied in Refs. [58,67]. The phase space determines the global behavior of the 2p2h responses, on top of the additional modifications introduced by the particular model of two-body current operator. The main modification of the phase-space behavior in the responses is produced by the Q^2 dependence of the electroweak form factors. The rest of the dependency on (q, ω) comes from the structure of the different Feynman diagrams, which are dominated by the forward Δ excitations.

In this work, we approximate the phase space using the frozen nucleon approximation [58,67], consisting in neglecting the momenta of the holes compared to the momentum transfer, which usually is larger than k_F . Setting $\mathbf{h}_1 = \mathbf{h}_2 = 0$, and $E_1 = E_2 = m_N^*$ inside the integral (47), one can perform the integral over $\mathbf{h}_1, \mathbf{h}_2$,

$$F(q, \omega)_{\text{frozen}} = \left(\frac{4}{3}\pi k_F^3\right)^2 \int d^3 p'_1 \frac{(m_N^*)^2}{E'_1 E'_2} \Theta(p'_1, 0) \times \Theta(p'_2, 0) \delta(E'_1 + E'_2 - 2m_N^* - \omega). \quad (48)$$

This integral can be reduced to one dimension, integrating over the momentum p'_1 and the azimuthal angle ϕ'_1 of the first ejected nucleon. In Ref. [58], the phase-space function (47) was studied by computing the seven-dimensional integral numerically and compared to the frozen approximation (48). This approximation is very good even for low momenta, except in the very low-energy threshold zone, where the 2p2h cross section is very small.

If we neglect Pauli blocking, the integral in Eq. (48) can be made analytically by going to the center-of-mass frame of the two final nucleons [67]. The following approximate formula is obtained:

$$F(q, \omega) \simeq F(q, \omega)_{\text{frozen}} \simeq 4\pi \left(\frac{4}{3}\pi k_F^3\right)^2 \frac{m_N^{*2}}{2} \sqrt{1 - \frac{4m_N^{*2}}{(2m_N^* + \omega)^2 - q^2}}. \quad (49)$$

From this equation, we obtain the minimum ω to excite a 2p2h state for fixed q , in this approximation,

$$\omega_{\min} = \sqrt{4m_N^{*2} + q^2} - 2m_N^*. \quad (50)$$

The phase-space integral is zero below this value. Note that this is the kinetic energy of a particle with mass $2m_N^*$ and momentum q .

E. Averaged Δ propagator

When a Δ is excited in the Δ -forward diagrams (f) and (g) of Fig. 1, a broad resonant peak is produced. This produces the dominant contribution to the MEC responses in the region around the Δ peak. To get this resonant peak in the semiempirical formula, we will approximate it by an average of the Δ propagator over the Fermi gas.

The peak of the 2p2h responses is due to the denominator in the Δ propagator for the forward diagrams,

$$G_\Delta(H + Q) \equiv \frac{1}{(H + Q)^2 - M_\Delta^2 + iM_\Delta\Gamma_\Delta + \frac{\Gamma_\Delta^2}{4}}, \quad (51)$$

where $H^\mu = (E_{\text{RMF}}, \mathbf{h})$ is the 4-momentum of the hole. The square of the momentum in the denominator can be written

$$(H + Q)^2 = (E_{\text{RMF}} + \omega)^2 - (\mathbf{h} + \mathbf{q})^2 \simeq (m_N^* + E_v + \omega)^2 - 2\mathbf{h} \cdot \mathbf{q} - q^2, \quad (52)$$

where the energy of the hole has been approximated by $E_{\text{RMF}} = m_N^* + E_v$ in the RMF model, by neglecting the kinetic energy of the first particle, and the momentum h^2

has also been neglected compared to the momentum transfer q^2 . In this nonrelativistic limit for the initial nucleon, an average of the propagator (51) can be computed analytically,

$$G_{\text{av}}(Q) = G_{\text{av}}(q, \omega) = \frac{1}{\frac{4}{3}\pi k_F^3} \int \frac{d^3 h \theta(k_F - |\mathbf{h}|)}{a - 2\mathbf{h} \cdot \mathbf{q} + ib}, \quad (53)$$

$$= \frac{1}{\frac{4}{3}\pi k_F^3 q} \left\{ \frac{(a+ib)k_F}{2q} + \frac{4q^2 k_F^2 - (a+ib)^2}{8q^2} \times \ln \left[\frac{a+2k_F q + ib}{a-2k_F q + ib} \right] \right\}, \quad (54)$$

where the functions a and b are defined by

$$a \equiv m_N^{*2} + (\omega + E_v)^2 - q^2 + 2m_N^*(\omega + E_v + \Sigma) - M_\Delta^2 + \frac{\Gamma_\Delta^2}{4} \quad (55)$$

$$b \equiv M_\Delta \Gamma_\Delta. \quad (56)$$

Note that we have included a shift parameter $\Sigma(q)$, to obtain the correct position of the smeared Δ peak. The Δ width Γ_Δ will be replaced by an effective width on the average $\Gamma(q)$.

The effective width and shift are used only in the averaged propagator. In the exact calculation of the MEC, there is no shift, and the well-known value of the width of the Delta $\Gamma_\Delta(Q^2)$ is used. In Ref. [41], it was shown that the averaged propagator (in Ref. [41], it was called the ‘‘frozen’’ propagator) describes the ω dependence of the 2p2h responses only if effective values of $\Gamma(q)$ and $\Sigma(q)$ are used. The effective values are taken as parameters in the semiempirical formula, and they are fitted to the exact responses. As explained in detail in Ref. [41], in the exact responses, the Δ propagator inside the seven-dimensional integral is being multiplied by a q -dependent weight determined by the matrix elements of the MEC. This changes the position and width of the MEC peak with respect to the simple average of the denominator.

The effective shift and width parameters, $\Sigma(q)$, and $\Gamma(q)$, will be adjusted with the semiempirical formula of the next section, for each value of the momentum transfer q .

III. SEMIEMPIRICAL FORMULAS OF MEC RESPONSES

In this section, we propose the semiempirical formulas for the nuclear responses, $R_K(q, \omega)$, by separating the contributions of the different Feynman diagrams of MEC and the interferences between them and extracting the contribution from the phase space, electroweak form factors, and coupling constants, corresponding to each term of the current. In the case of the Δ -forward current, we also extract an average value of the Δ propagator. Much

of the dependence on q and ω is coming from these factors. The remaining dependence is coded into coefficients $\tilde{C}_i(q)$ that are assumed to only depend on q .

First, we write the MEC as

$$j^\mu = j_{\text{SP}}^\mu + j_{\Delta F}^\mu + j_{\Delta B}^\mu, \quad (57)$$

where the seagull-pionic (SP) contribution is the sum of Figs. 1(a)–1(e),

$$j_{\text{SP}}^\mu = j_{\text{sea}}^\mu + j_\pi^\mu + j_{\text{pole}}^\mu. \quad (58)$$

Now, to compute the hadronic tensor $w^{\mu\nu}$, Eq. (25), we deal with products of the kind

$$j^{\mu*} j^\nu = j_{\text{SP}}^{\mu*} j_{\text{SP}}^\nu + j_{\Delta F}^{\mu*} j_{\Delta F}^\nu + j_{\Delta B}^{\mu*} j_{\Delta B}^\nu + j_{\text{SP}}^{\mu*} j_{\Delta F}^\nu + j_{\Delta F}^{\mu*} j_{\text{SP}}^\nu + j_{\text{SP}}^{\mu*} j_{\Delta B}^\nu + j_{\Delta B}^{\mu*} j_{\text{SP}}^\nu + j_{\Delta F}^{\mu*} j_{\Delta B}^\nu + j_{\Delta B}^{\mu*} j_{\Delta F}^\nu. \quad (59)$$

Using this expansion, the response functions (7)–(11) can be written as the sum of six subresponses corresponding to SP, ΔF , and ΔB , plus the interferences $\Delta F - \text{SP}$, $\Delta B - \text{SP}$, and $\Delta F - \Delta B$,

$$R^K(q, \omega) = R_{\text{SP}}^K + R_{\Delta F}^K + R_{\Delta B}^K + R_{\Delta F-\text{SP}}^K + R_{\Delta B-\text{SP}}^K + R_{\Delta F-\Delta B}^K; \quad (60)$$

this is a general expansion for all responses. In the case of the CC , CL , LL , and T responses, we can also separate the contribution of the vector and axial parts of the current,

$$R^K(q, \omega) = R^{K,VV} + R^{K,AA}, \quad K = CC, CL, LL, T, \quad (61)$$

and their expansion is

$$R^{K,VV}(q, \omega) = R_{\text{SP}}^{K,VV} + R_{\Delta F}^{K,VV} + R_{\Delta B}^{K,VV} + R_{\Delta F-\text{SP}}^{K,VV} + R_{\Delta B-\text{SP}}^{K,VV} + R_{\Delta F-\Delta B}^{K,VV} \quad (62)$$

$$R^{K,AA}(q, \omega) = R_{\text{SP}}^{K,AA} + R_{\Delta F}^{K,AA} + R_{\Delta B}^{K,AA} + R_{\Delta F-\text{SP}}^{K,AA} + R_{\Delta B-\text{SP}}^{K,AA} + R_{\Delta F-\Delta B}^{K,AA}. \quad (63)$$

In the case of the T' response, only the vector-axial product contributes,

$$R^{T'}(q, \omega) = R^{T',VA}(q, \omega) = R_{\text{SP}}^{T',VA} + R_{\Delta F}^{T',VA} + R_{\Delta B}^{T',VA} + R_{\Delta F-\text{SP}}^{T',VA} + R_{\Delta B-\text{SP}}^{T',VA} + R_{\Delta F-\Delta B}^{T',VA}. \quad (64)$$

We have written the 2p2h response functions as sums of the subresponses vector-vector, $R_{I,J}^{K,VV}$; axial-axial, $R_{I,J}^{K,AA}$; and vector-axial, $R_{I,J}^{T',VA}$, with $I, J = \text{SP}, \Delta F, \Delta B$. From each one of these subresponses, we factorize the electroweak form factors, the coupling constants, an average delta propagator $G_{\text{av}}(q, \omega)$ for each ΔF current, and finally the phase space $\frac{V}{(2\pi)^9} F(q, \omega)$. Then, for each subresponse, we propose a semiempirical formula. Schematically, the general structure will be

$$R_i(q, \omega) = [\text{phase-space}] \times [\text{coupling constants}] \times [\text{form factors}] \times [\text{averaged } \Delta \text{ propagators}] \times \tilde{C}_i(q), \quad (65)$$

where we assume that the adjustable coefficients $\tilde{C}_i(q)$ do not depend on ω , but only depend on q . This is the main hypothesis on which the parametrization is based, that is, that most of the ω dependence comes from phase space, form factors, and the averaged Δ propagator. This is justified *a posteriori* in the next section when we check the quality of the fit by comparison with the exact results. These coefficients will be fitted to the corresponding subresponses in an exact calculation. The coefficients can be interpreted as nuclear mean values of spin-isospin contributions of the Feynman diagrams for each subresponse in a 2p2h excitation.

Below, we write down the explicit formula for the 54 subresponses, taking into account that some of them may need two coefficients or some additional correction, which will be discussed in the next section.

A. Response R_T^{VV}

$$R_{\Delta F}^{T,VV} = \frac{V}{(2\pi)^9} F(q, \omega) \left(\frac{f^* f_{\pi NN}}{m_\pi^2} \right)^2 \left(\frac{C_3^V}{m_N} \right)^2 [\tilde{C}_{1,V1}(\text{Re}(G_{\text{av}}^V))^2 + \tilde{C}_{1,V2}(\text{Im}(G_{\text{av}}^V))^2] (m_N^4) \quad (66)$$

$$R_{\text{SP}}^{T,VV} = \frac{V}{(2\pi)^9} F(q, \omega) \left(\frac{f_{\pi NN}^2}{m_\pi^2} \right)^2 (F_1^V)^2 (\tilde{C}_{2,V} \cdot m_N^{-2}) \left[1 - \frac{\omega - 0.7q}{m_N} \right]^2 \quad (67)$$

$$R_{\Delta B}^{T,VV} = \frac{V}{(2\pi)^9} F(q, \omega) \left(\frac{f^* f_{\pi NN}}{m_\pi^2} \right)^2 \left(\frac{C_3^V}{m_N} \right)^2 (\tilde{C}_{3,V}) \quad (68)$$

$$R_{\Delta F-SP}^{T,VV} = \frac{V}{(2\pi)^9} F(q, \omega) \left(\frac{f^* f_{\pi NN}^3}{m_\pi^4} \right) \left(\frac{C_3^V}{m_N} \right) (F_1^V) [\tilde{C}_{4,V1}(\text{Re}(G_{av}^V)) + \tilde{C}_{4,V2}(\text{Im}(G_{av}^V))] (m_N) \quad (69)$$

$$R_{\Delta F-\Delta B}^{T,VV} = \frac{V}{(2\pi)^9} F(q, \omega) \left(\frac{f^* f_{\pi NN}}{m_\pi^2} \right)^2 \left(\frac{C_3^V}{m_N} \right)^2 [\tilde{C}_{5,V1}(\text{Re}(G_{av}^V)) + \tilde{C}_{5,V2}(\text{Im}(G_{av}^V))] (m_N^2) \quad (70)$$

$$R_{\Delta B-SP}^{T,VV} = \frac{V}{(2\pi)^9} F(q, \omega) \left(\frac{f^* f_{\pi NN}^3}{m_\pi^4} \right) \left(\frac{C_3^V}{m_N} \right) (F_1^V) (\tilde{C}_{6,V} \cdot m_N^{-1}) \quad (71)$$

B. Response R_T^{AA}

$$R_{\Delta F}^{T,AA} = \frac{V}{(2\pi)^9} F(q, \omega) \left(\frac{f^* f_{\pi NN}}{m_\pi^2} \right)^2 (C_5^A)^2 [\tilde{C}_{1,A1}(\text{Re}(G_{av}^A))^2 + \tilde{C}_{1,A2}(\text{Im}(G_{av}^A))^2] (m_N^2) \quad (72)$$

$$R_{SP}^{T,AA} = \frac{V}{(2\pi)^9} F(q, \omega) \left(\frac{f_{\pi NN}^2}{m_\pi^2} \right)^2 \left(\frac{1}{g_A} \right)^2 (\tilde{C}_{2,A} \cdot m_N^{-2}) \quad (73)$$

$$R_{\Delta B}^{T,AA} = \frac{V}{(2\pi)^9} F(q, \omega) \left(\frac{f^* f_{\pi NN}}{m_\pi^2} \right)^2 (C_5^A)^2 (\tilde{C}_{3,A} \cdot m_N^{-2}) \quad (74)$$

$$R_{\Delta F-SP}^{T,AA} = \frac{V}{(2\pi)^9} F(q, \omega) \left(\frac{f^* f_{\pi NN}^3}{m_\pi^4} \right) (C_5^A) \left(\frac{1}{g_A} \right) [\tilde{C}_{4,A1}(\text{Re}(G_{av}^A)) + \tilde{C}_{4,A2}(\text{Im}(G_{av}^A))] \quad (75)$$

$$R_{\Delta F-\Delta B}^{T,AA} = \frac{V}{(2\pi)^9} F(q, \omega) \left(\frac{f^* f_{\pi NN}}{m_\pi^2} \right)^2 (C_5^A)^2 [\tilde{C}_{5,A1}(\text{Re}(G_{av}^A)) + \tilde{C}_{5,A2}(\text{Im}(G_{av}^A))] \quad (76)$$

$$R_{\Delta B-SP}^{T,AA} = \frac{V}{(2\pi)^9} F(q, \omega) \left(\frac{f^* f_{\pi NN}^3}{m_\pi^4} \right) (C_5^A) \left(\frac{1}{g_A} \right) (\tilde{C}_{6,A} \cdot m_N^{-2}) \quad (77)$$

C. Response R_T^{VA}

$$R_{\Delta F}^{T',VA} = \frac{V}{(2\pi)^9} F(q, \omega) \left(\frac{f^* f_{\pi NN}}{m_\pi^2} \right)^2 \left(\frac{C_3^V}{m_N} \right) (C_5^A) [\tilde{C}_{1,VA1}(\text{Re}(G_{av}^{VA}))^2 + \tilde{C}_{1,VA2}(\text{Im}(G_{av}^{VA}))^2] (m_N^3) \quad (78)$$

$$R_{SP}^{T',VA} = \frac{V}{(2\pi)^9} F(q, \omega) \left(\frac{f_{\pi NN}^2}{m_\pi^2} \right)^2 (F_1^V) \left(\frac{1}{g_A} \right) (\tilde{C}_{2,VA} \cdot m_N^{-2}) \left[1 - \frac{\omega - 0.7q}{m_N} \right]^2 \quad (79)$$

$$R_{\Delta B}^{T',VA} = \frac{V}{(2\pi)^9} F(q, \omega) \left(\frac{f^* f_{\pi NN}}{m_\pi^2} \right)^2 \left(\frac{C_3^V}{m_N} \right) (C_5^A) (\tilde{C}_{3,VA} \cdot m_N^{-1}) \quad (80)$$

$$R_{\Delta F-SP}^{T',VA} = \frac{V}{(2\pi)^9} F(q, \omega) \left(\frac{f^* f_{\pi NN}^3}{m_\pi^4} \right) |G_{av}^{VA}| \left[\left(\frac{C_3^V}{m_N} \right) \left(\frac{1}{g_A} \right) (\tilde{C}_{4,VA1} \cdot m_N) + (C_5^A) (F_1^V) (\tilde{C}_{4,VA2}) \right] \quad (81)$$

$$R_{\Delta F-\Delta B}^{T',VA} = \frac{V}{(2\pi)^9} F(q, \omega) \left(\frac{f^* f_{\pi NN}}{m_\pi^2} \right)^2 \left(\frac{C_3^V}{m_N} \right) (C_5^A) [\tilde{C}_{5,VA1}(\text{Re}(G_{av}^{VA})) + \tilde{C}_{5,VA2}(\text{Im}(G_{av}^{VA}))] 2m_N \quad (82)$$

$$R_{\Delta B-SP}^{T',VA} = \frac{V}{(2\pi)^9} F(q, \omega) \left(\frac{f^* f_{\pi NN}^3}{m_\pi^4} \right) \left[\left(\frac{C_3^V}{m_N} \right) \left(\frac{1}{g_A} \right) (\tilde{C}_{6,VA} \cdot m_N^{-1}) + (C_5^A) (F_1^V) (\tilde{C}_{6,AV} \cdot m_N^{-2}) \right] \quad (83)$$

D. Response R_{CC}^{VV}

$$R_{\Delta F}^{CC,VV} = \frac{V}{(2\pi)^9} F(q, \omega) \left(\frac{f^* f_{\pi NN}}{m_\pi^2} \right)^2 \left(\frac{C_3^V}{m_N} \right)^2 [\tilde{C}_{1,V1} (\text{Re}(G_{\text{av}}^V))^2 + \tilde{C}_{1,V2} (\text{Im}(G_{\text{av}}^V))^2] (m_N^4) \quad (84)$$

$$R_{SP}^{CC,VV} = \frac{V}{(2\pi)^9} F(q, \omega) \left(\frac{f_{\pi NN}^2}{m_\pi^2} \right)^2 (F_1^V)^2 (\tilde{C}_{2,V} \cdot m_N^{-2}) \quad (85)$$

$$R_{\Delta B}^{CC,VV} = \frac{V}{(2\pi)^9} F(q, \omega) \left(\frac{f^* f_{\pi NN}}{m_\pi^2} \right)^2 \left(\frac{C_3^V}{m_N} \right)^2 (\tilde{C}_{3,V}) \quad (86)$$

$$R_{\Delta F-SP}^{CC,VV} = \frac{V}{(2\pi)^9} F(q, \omega) \left(\frac{f^* f_{\pi NN}^3}{m_\pi^4} \right) \left(\frac{C_3^V}{m_N} \right) (F_1^V) [\tilde{C}_{4,V1} (\text{Re}(G_{\text{av}}^V)) + \tilde{C}_{4,V2} (\text{Im}(G_{\text{av}}^V))] (m_N) \quad (87)$$

$$R_{\Delta F-\Delta B}^{CC,VV} = \frac{V}{(2\pi)^9} F(q, \omega) \left(\frac{f^* f_{\pi NN}}{m_\pi^2} \right)^2 \left(\frac{C_3^V}{m_N} \right)^2 [\tilde{C}_{5,V1} (\text{Re}(G_{\text{av}}^V)) + \tilde{C}_{5,V2} (\text{Im}(G_{\text{av}}^V))] (m_N^2) \quad (88)$$

$$R_{\Delta B-SP}^{CC,VV} = \frac{V}{(2\pi)^9} F(q, \omega) \left(\frac{f^* f_{\pi NN}^3}{m_\pi^4} \right) \left(\frac{C_3^V}{m_N} \right) (F_1^V) (\tilde{C}_{6,V} \cdot m_N^{-1}) \quad (89)$$

E. Response R_{CC}^{AA}

$$R_{\Delta F}^{CC,AA} = \frac{V}{(2\pi)^9} F(q, \omega) \left(\frac{f^* f_{\pi NN}}{m_\pi^2} \right)^2 (C_5^A)^2 [\tilde{C}_{1,A1} (\text{Re}(G_{\text{av}}^A))^2 + \tilde{C}_{1,A2} (\text{Im}(G_{\text{av}}^A))^2] (m_N^2) \quad (90)$$

$$R_{SP}^{CC,AA} = \frac{V}{(2\pi)^9} F(q, \omega) \left(\frac{f_{\pi NN}^2}{m_\pi^2} \right)^2 \left(\frac{1}{g_A} \right)^2 \left[\tilde{C}_{2,A1} + \tilde{C}_{2,A2} \left(\frac{\omega \cdot m_N}{Q^2 - m_\pi^2} \right)^2 \right] (m_N^{-2}) \quad (91)$$

$$R_{\Delta B}^{CC,AA} = \frac{V}{(2\pi)^9} F(q, \omega) \left(\frac{f^* f_{\pi NN}}{m_\pi^2} \right)^2 (C_5^A)^2 (\tilde{C}_{3,A} \cdot m_N^{-2}) \quad (92)$$

$$R_{\Delta F-SP}^{CC,AA} = \frac{V}{(2\pi)^9} F(q, \omega) \left(\frac{f^* f_{\pi NN}^3}{m_\pi^4} \right) (C_5^A) \left(\frac{1}{g_A} \right) [\tilde{C}_{4,A1} (\text{Re}(G_{\text{av}}^A)) + \tilde{C}_{4,A2} (\text{Im}(G_{\text{av}}^A))] \quad (93)$$

$$R_{\Delta F-\Delta B}^{CC,AA} = \frac{V}{(2\pi)^9} F(q, \omega) \left(\frac{f^* f_{\pi NN}}{m_\pi^2} \right)^2 (C_5^A)^2 [\tilde{C}_{5,A1} (\text{Re}(G_{\text{av}}^A)) + \tilde{C}_{5,A2} (\text{Im}(G_{\text{av}}^A))] \quad (94)$$

$$R_{\Delta B-SP}^{CC,AA} = \frac{V}{(2\pi)^9} F(q, \omega) \left(\frac{f^* f_{\pi NN}^3}{m_\pi^4} \right) (C_5^A) \left(\frac{1}{g_A} \right) (\tilde{C}_{6,A} \cdot m_N^{-2}) \quad (95)$$

F. Responses R_{CL}^{VV} and R_{LL}^{VV}

These responses are computed assuming conservation of the vector current:

$$R_{CL}^{VV} = -\frac{\omega}{q} R_{CC}^{VV} \quad (96)$$

$$R_{LL}^{VV} = \frac{\omega^2}{q^2} R_{CC}^{VV} \quad (97)$$

G. Responses R_{CL}^{AA} and R_{LL}^{AA}

The semiempirical formulas for R_{CL}^{AA} and R_{LL}^{AA} are similar to the R_{CC}^{AA} . Only the numerical values of the coefficients \tilde{C}_i change.

H. Electromagnetic responses R_{em}^L and R_{em}^T

It can be shown with the formalism of Ref. [66] that for symmetric nuclear matter the electromagnetic 2p2h responses are one-half of the VV weak responses

$$R_{em}^L = \frac{1}{2} R^{CC,VV} \quad (98)$$

$$R_{em}^T = \frac{1}{2} R^{T,VV}. \quad (99)$$

Therefore, the same semiempirical formulas for the VV responses apply for the electromagnetic responses with a factor 1/2.

I. Properties of semiempirical formulas

Here, we describe and clarify some particularities about the semiempirical formulas (66)–(95) for the subresponses and their theoretical meaning:

- (i) All the dependence on ω is analytical. So, the semiempirical expansion assumes that the ω dependence comes mainly from the product of phase space $F(q, \omega)$, electroweak form factors, and averaged Δ propagator. The only exceptions are $R_{SP}^{T,VV}$ and $R_{SP}^{T,VA}$ subresponses, which include an ω -dependent factor that is obtained empirically by comparing with the exact result.
- (ii) The coefficients \tilde{C}_i in all the formulas are dimensionless. That is why powers of nucleon masses have been introduced in the subresponses.
- (iii) The phase space $F(q, \omega)$ is common to all the formulas. In this work, it is computed analytically using the approximation (49).
- (iv) All the responses are proportional to the volume $V = (2\pi)^3 Z / (\frac{8}{3} \pi k_F^3)$ for symmetric nuclear matter $Z = N$. For asymmetric matter, the formulas should be modified using two different Fermi momenta for protons and neutrons.
- (v) Each subresponse includes a specific product of form factors and coupling constants, except the axial SP subresponses, which do not allow us to extract explicitly the form factor $F_\rho(k_i)$.
- (vi) In most subresponses, the averaged Δ propagator appears separated in real and imaginary parts, each one multiplied by a parameter \tilde{C}_i . The only exception is the $R_{\Delta F-SP}^{T,VA}$, which only include the modulus $|G_{av}|$. Note that in the formulas there are three versions of the averaged propagator: G_{av}^V for the VV responses, G_{av}^A for the AA subresponses,

and G_{av}^{VA} for the T' , VA responses. They differ in the values of the effective width, Γ , and shift, Σ , of the Δ propagator. The corresponding six parameters are denoted by Γ_V , Γ_A , Γ_{VA} , Σ_V , Σ_A , and Σ_{VA} .

Finally, the semiempirical formulas allow us to calculate analytically and directly all the 2p2h electroweak responses. For a fixed value of q , the total 2p2h response depends on the sum of all the subresponses, with a total of 73 parameters. This number of parameters may seem large. Note that the axial part and the vector part of the five response functions, as well as their interferences, are described simultaneously. This could be compared with the parametrization of Refs. [20,46], which needs about 56 parameters to describe all the 2p2h responses in another nuclear model, based on the RFG and not RMF, and also using only the real part of the Δ propagator. Here, we use the full Δ propagator [53]. However, the present parametrization is an advance since we obtain explicit dependence of the responses on physical magnitudes—form factors, coupling constants, Fermi momentum, etc—that can be modified *a posteriori* if desired. Also, as we show below, many of these 54 subresponses are very small and could safely neglected, leaving us with a smaller number of parameters. However, in this paper, we have computed all the subresponses.

IV. RESULTS

In this section, we obtain the values of the coefficients of the semiempirical formulas (66)–(95) and the parameters Γ and Σ in the averaged Δ propagator (54), (55), (56). Since the experimental responses are not available and it is not possible to obtain them phenomenologically, the coefficients cannot be obtained directly from data. Therefore, the only possibility is to fit a theoretical model. In our case, the interest is to obtain a parametrization of the responses to make theoretical predictions of neutrino cross sections in a computationally fast way. All numerical results in this section correspond to ^{12}C with $k_F = 225$ MeV/ c , $M^* = 0.8$, and $E_\nu = 141$ MeV, fitted in Ref. [53].

First, we have calculated the “exact” subresponses for a set of kinematics, (q, ω) , performing numerical integrations in seven dimensions in the RMF of nuclear matter described in Sec. II. Our computer code calculates the seven total 2p2h responses of neutrino CC scattering, R_K , $K = CC, CL, LL, T, T'$, and electrons, R_{em}^L and R_{em}^T , using Eq. (27). Our numerical code allows us to include in the calculation some specific Feynman diagrams and exclude others. To compute the subresponses, we have performed three runs with the individual currents, SP, ΔF , and ΔB , and three more runs with the pairs of currents (SP + ΔF), (SP + ΔB), and (ΔF + ΔB). Subtracting the separate contributions of the single currents, the interference subresponses are obtained. For instance,

$$R_{\text{SP}-\Delta F} = R_{\text{SP}+\Delta F} - R_{\text{SP}} - R_{\Delta F}. \quad (100)$$

An additional run is performed with the full MEC to get the complete result. Each run requires computing the seven response functions in a grid of (q, ω) values, with $q = 200, \dots, 2000$ MeV/c in steps of $\Delta q = 100$ and $\omega = 10, \dots, q$ in steps of $\Delta \omega = 10$ MeV. The grid contains about 15,000 kinematical points (q_i, ω_i) . Note that the computation for each kinematical point takes an average of 5 min on our high-performance processors. This means each run requires about 52 days in one processor and one year for the seven runs. We have used the PROTEUS scientific computing cloud of the ic1 [68] [2300 processors with total 90,000 Giga FLOP (floating point arithmetic operations)], allowing us to do the calculation in a few days.

Once we have stored the tables of the exact subresponses in the grid, we fit the coefficients of the semiempirical

formula for fixed q . The fit is made by minimizing a χ^2 function for each subresponse separately, thus obtaining the coefficients $\tilde{C}_i(q)$. The $R_{\Delta F}^{T,VV}$ responses are used to fit the effective width, $\Gamma_V(q)$, and shift, $\Sigma_V(q)$, of the averaged delta propagator as well. The same procedure is followed to fit the AA and VA effective widths and shifts using the responses $R_{\Delta F}^{T,AA}$, and $R_{\Delta F}^{T,VA}$, respectively. Therefore, in the transverse subresponses ΔF , four coefficients are being adjusted simultaneously. Once the widths and shifts have been fitted in this way, they are set to that value in all the subresponses.

The coefficients obtained in the fit are tabulated in Appendix B. In Table I, the effective width, $\Gamma(q)$, and shift, $\Sigma(q)$, of the averaged Δ propagator, $G_{\text{av}}(q, \omega)$, are given for VV, AA, or VA responses. The coefficients \tilde{C}_i are provided in Tables II (for the R_T^{VV} response function),

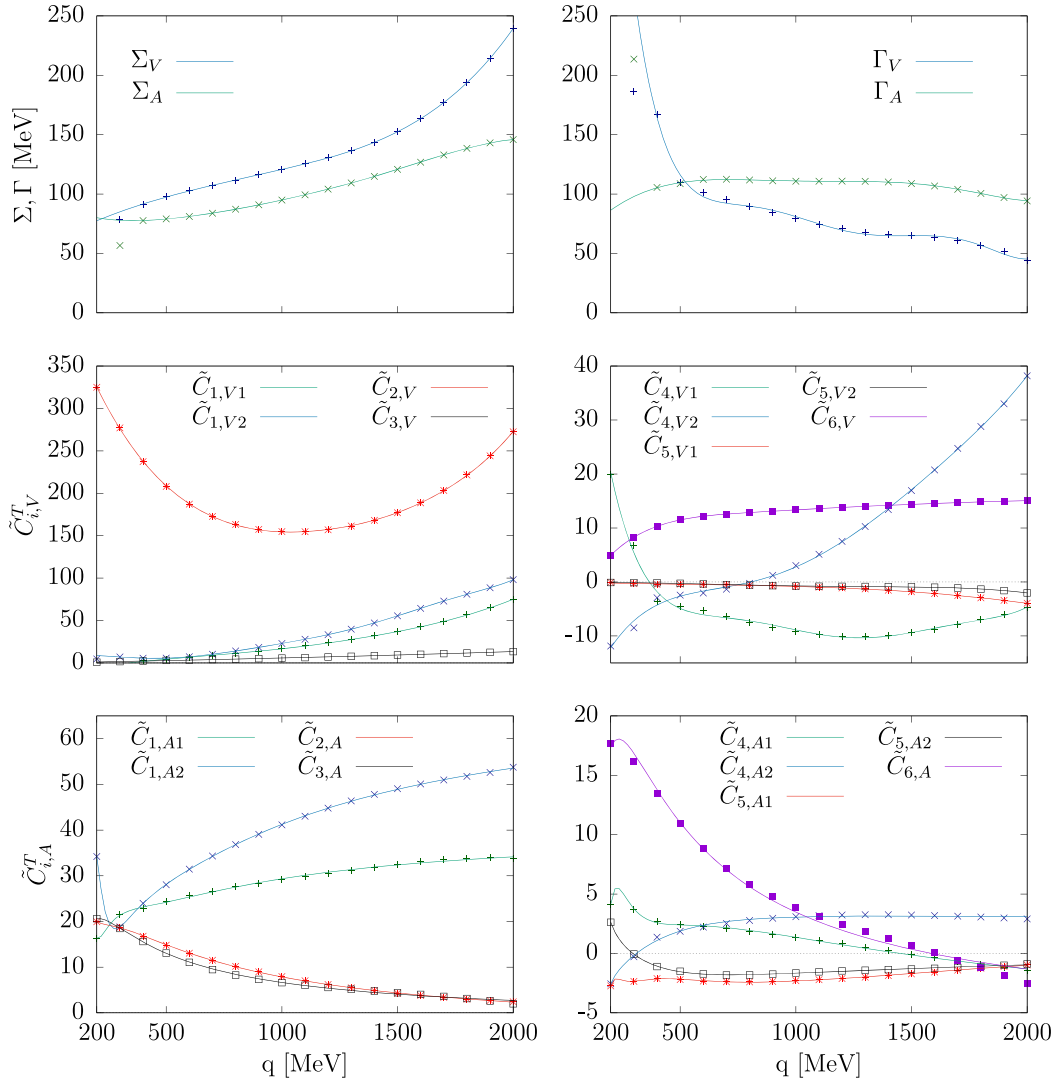


FIG. 2. Coefficients of the semiempirical formulas and parameters Γ, Σ in the averaged Δ propagator, for the R^T 2p2h response function plotted against the momentum transfer q . The dots are the fitted values, and the curves are the parametrizations with polynomial functions. Tables of these coefficients and parametrizations are given in the Appendix.

III (for R_T^{AA}), IV (for R_{CC}^{VV}), V (for R_{CC}^{AA}), VI (for R_{CL}^{AA}), VII (for R_{LL}^{AA}), and VIII (for $R_{T'}^A$). The tables are given as a function of q and can be interpolated for other q values. We also provide polynomial parametrizations in Appendix C.

In Fig. 2, we plot the coefficients of the semiempirical formula for the case of the subresponses R^T for VV and AA cases. We plot the coefficients \tilde{C}_i and the effective widths, Γ_V and Γ_A , and shifts, Σ_V and Σ_A , of the averaged Δ propagator as a function of the momentum transfer q . Smooth dependence on q is observed, except for very low q below 300 MeV/c where the dependence is more abrupt in some cases, specifically in the case of the widths and shifts of the Δ propagator for $q < 300$ MeV/c. The reason why there is an abrupt change for low momentum in the Δ current

coefficients is because the peak of the delta is not reached below $q = 300$ MeV/c, since at least the transferred energy must be large enough to produce the Δ . In the present RMF model, this is $\omega = m_\Delta - m_N^* - E_v \simeq 340$ MeV. Therefore, these coefficients are less restricted, and their value has greater indeterminacy when making the fit. Similar results—not shown in Fig. 2—are obtained for the dependence on q of the rest of the coefficients of the semiempirical formula.

The most relevant coefficients for calculating the responses are those corresponding to the Δ -forward transverse responses (T and T') because these subresponses are dominant in the Δ region. These coefficients are \tilde{C}_{1Vi} , \tilde{C}_{1Ai} , and \tilde{C}_{1VAi} . They increase moderately with q , and their values vary between $\tilde{C}_i \simeq 0$ and 100 for $200 \leq q \leq 2000$ MeV/c.

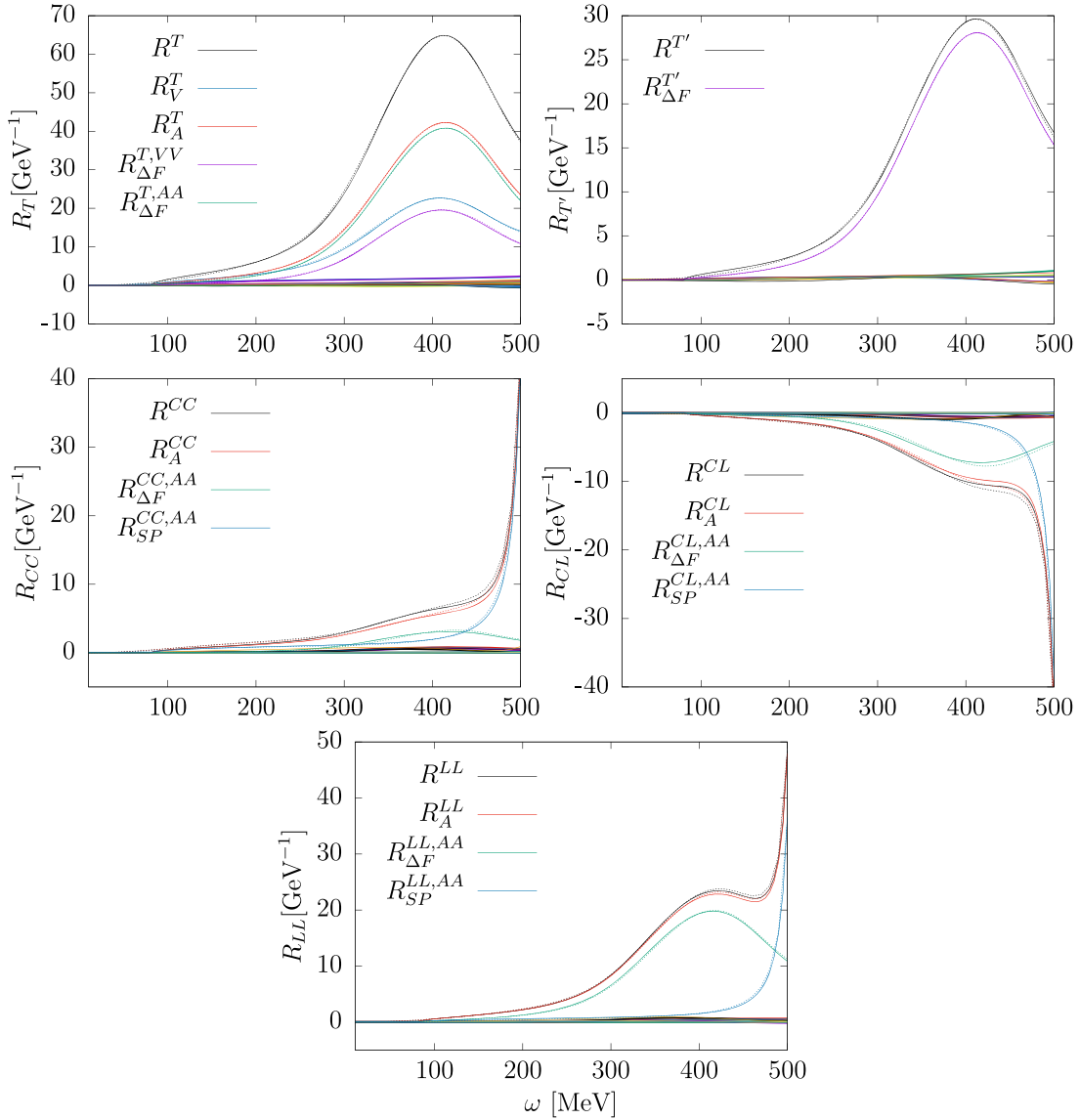


FIG. 3. Comparison between all the subresponses that contribute to each of the response functions for $q = 500$ MeV/c. Only the most important subresponses appear in the legend. But they are all drawn. For each color, the solid line is the parametrization, and the dotted lines are the exact calculation.

In Figs. 3 and 4, we show, as an example, all the responses and subresponses as a function of ω for two values of the momentum transfer $q = 500$ and 1000 MeV/c, respectively. The dominant subresponses in the responses T and T' are the delta-forward ones, while the axial delta-forward and seagull-pionic response functions CC , CL , and LL . The rest of the subresponses give a very small contribution to the total and could in principle be neglected, although we have included all in the calculation. In the figures, we plot the exact result and semiempirical formula, using the parametrization of the \tilde{C}_i parameters given in the Appendix C, for each one of the dominant subresponses and also for the total responses.

In Fig. 5, it is seen that the total responses are well described by the semiempirical formula in the range of $q = 200, \dots, 2000$ MeV/c considered in the present work. The

five 2p2h response functions for CC neutrino scattering from ^{12}C , computed with the RMF model and with the semiempirical formula, are mostly identical in the scale of the figure. This indicates that the semiempirical formula can be used with guarantees to calculate the cross section in the 2p2h channel. For other values of q , it is enough to interpolate the tables of the coefficients of Appendix B, or to use the polynomial parametrizations of Appendix C. In Fig. 6, we give an example of how the formula works in the case of (e, e') cross section of ^{12}C for various kinematics. The electron energy and the scattering angle are fixed in the experiment. When changing omega, the momentum transfer is not constant but depends on the three variables continuously. Then, it is necessary to interpolate the coefficients of the semiempirical formula to calculate the 2p2h cross section. In the figure, we used polynomial interpolation.

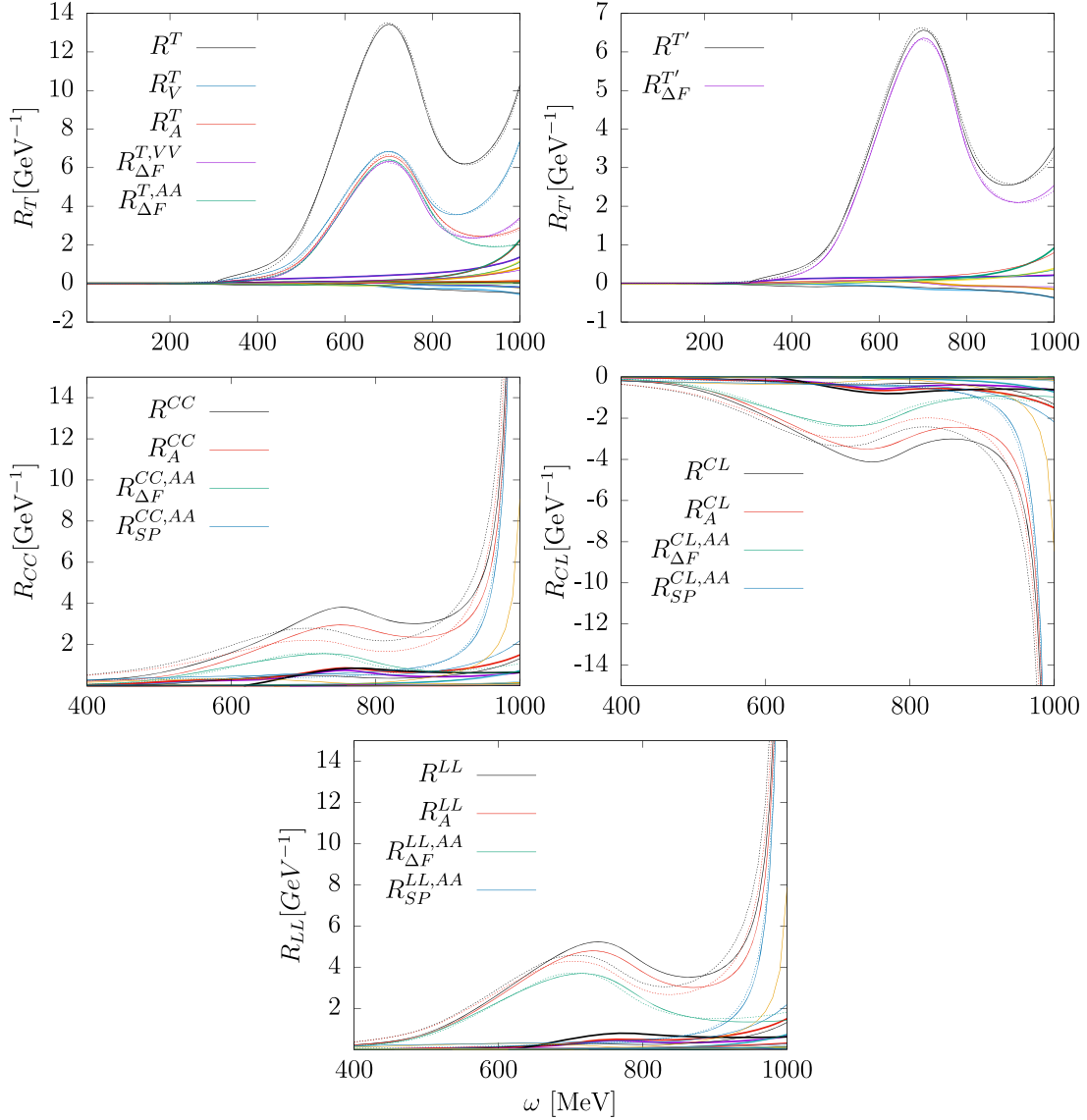


FIG. 4. The same as Fig. 3 for $q = 1000$ MeV/c.

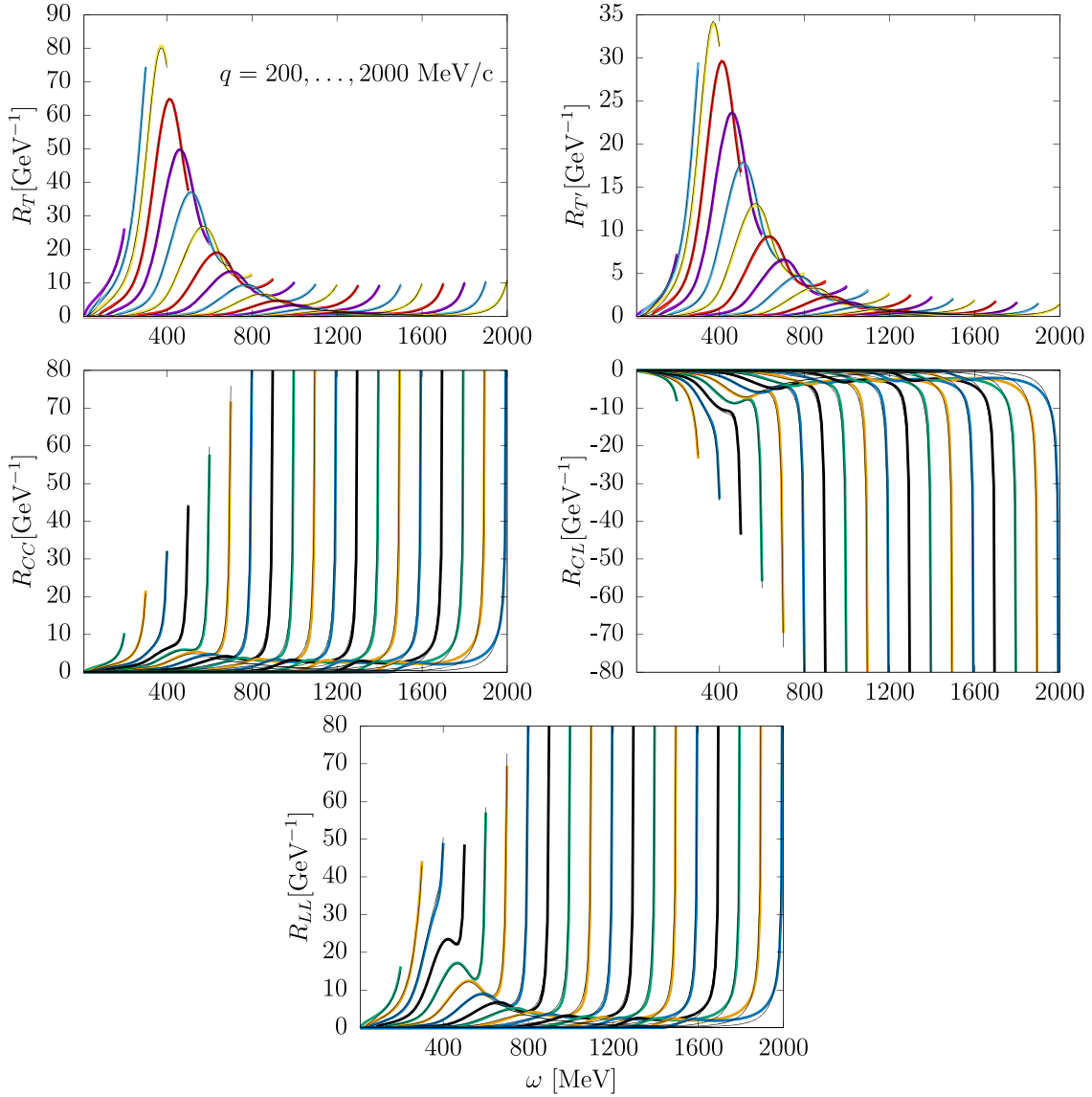


FIG. 5. Comparison of the five 2p2h response functions for CC neutrino scattering from ^{12}C , computed with the RMF model and with the semiempirical formula. They are plotted as a function of ω for fixed values of their momentum transfer $q = 200, \dots, 2000$ MeV/c.

The greatest utility of the SE formula is to calculate the 2p2h interaction with neutrinos, since the neutrino flux implies an integration on the incident energy. The integrated cross section in the flux is shown in Fig. 7. There, we show the transverse and longitudinal contributions to the cross section with and without 2p2h MEC. The effect of MEC responses, computed with the SE formula, is to increase the cross section of about $\sim 20\%$, depending on the kinematics. Note that these results have been obtained using $C_A^5(0) = 1.2$ for the axial Δ coupling. But in Ref. [59], it was found that a value of 0.89 was more adequate according to the pion emission data. If this value is used with the semiempirical formula, the effect of the axial MEC contribution in Fig. 7 would be reduced by almost one-half. Note that the L contribution of the MEC is

very small and almost negligible and could be omitted in the calculation.

To visualize the quality of the semiempirical formulas, we show in Fig. 8 the quotient between the semiempirical formula (se) and the exact result (th), for $q = 500$ MeV/c as a function of ω . In the zones dominated by the transverse responses T and T' at the peak of the delta, the quotient is very close to 1. For the ω values where the responses are appreciable, the quotient is practically 1 because the coefficients have been adjusted. The quotient deviates from 1 only for ω values where the responses are not important nor negligible.

The semiempirical formula also allows studying the relative behavior between the different contributions or subresponses. In particular, one can find relations between

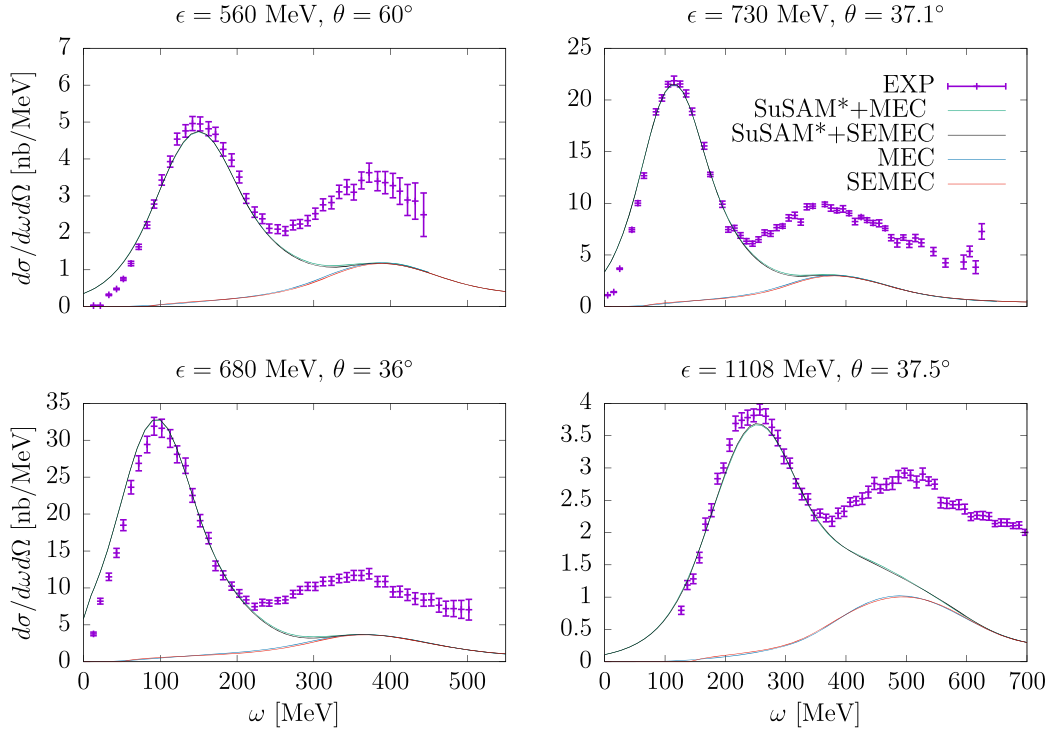


FIG. 6. Cross section for (e, e') scattering off ^{12}C for various kinematics as a function of omega. The quasielastic contribution with emission of a particle is shown using the SuSAM* model of Ref. [53] and the contribution of channel 2p2h, calculated both with the exact RMF (MEC) and with the semiempirical formula (SE-MEC). Experimental data are from Refs. [69–71].

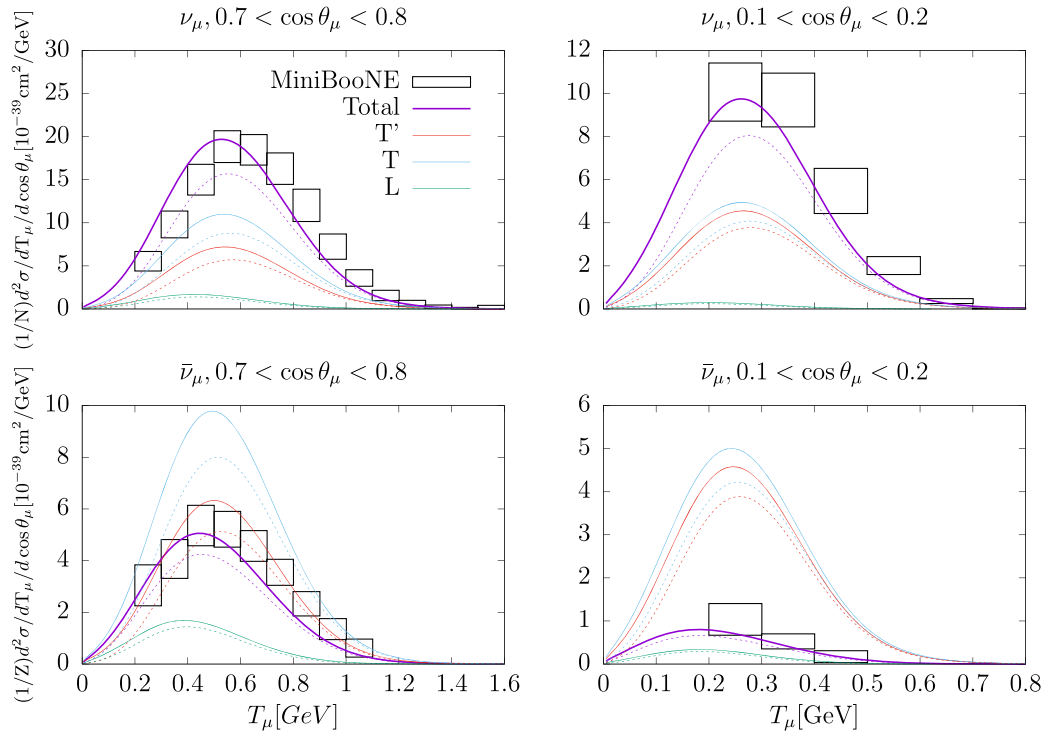


FIG. 7. Quasielastic neutrino and antineutrino, differential cross section integrated over the neutrino flux of the MiniBooNE experiment for selected kinematics of the scattering angle bins. we show the separate T , T' and longitudinal responses ($L = \text{CC} + \text{CL} + \text{LL}$) with and without MEC. The curves without MEC (dotted lines) have been computed using the SuSAM* model of Ref. [53]. The curves with MEC (solid lines) have been calculated with the SE formula of the 2p2h responses. Experimental data from Refs. [11,12].

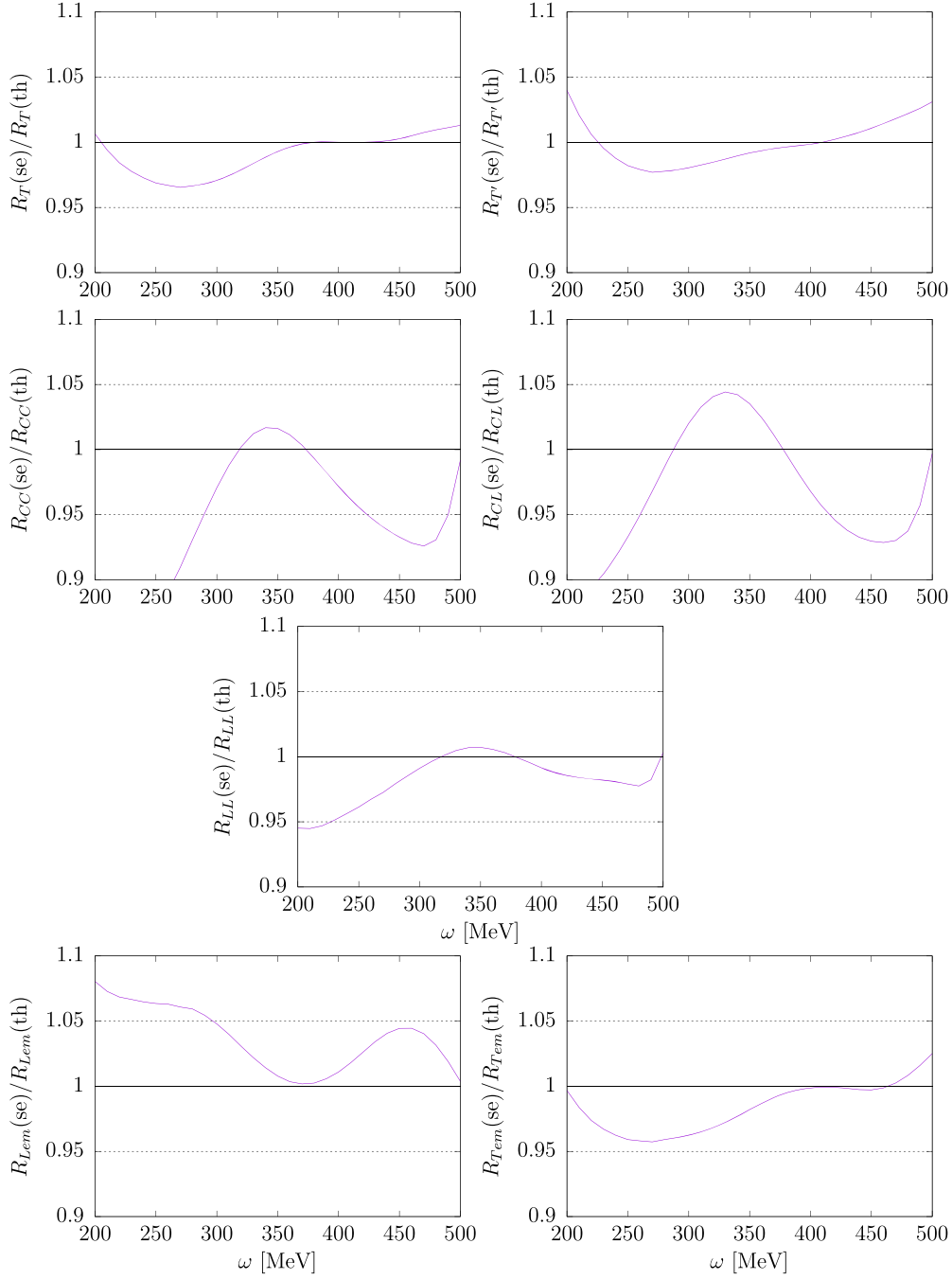


FIG. 8. Quotient between the semi-empirical (se) and theoretical (th) 2p2h response functions for CC neutrino and electron scattering. For $q = 500$ MeV/c as a function of ω .

the dominant subresponses $R_{\Delta F}^{TVV}$, $R_{\Delta F}^{T'VA}$, and $R_{\Delta F}^{TAA}$ as follows. First, note that the only difference between the vector and axial parts of the ΔF current, Eq. (31), is in the electroweak vertex (41), $\Gamma^{\beta\mu}(Q) = \Gamma_V^{\beta\mu}(Q) + \Gamma_A^{\beta\mu}(Q)$, with

$$\begin{aligned} \Gamma_V^{\beta\mu}(Q) &= \frac{C_3^V}{m_N} (g^{\beta\mu} \not{Q} - Q^\beta \gamma^\mu) \gamma_5, \\ \Gamma_A^{\beta\mu}(Q) &= C_5^A g^{\beta\mu}, \end{aligned} \quad (101)$$

Then, the vector current ΔF is expected to behave roughly like q/m with respect to the axial current. As a consequence, the coefficients of the semiempirical $R_{\Delta F}^{TVV}$ and $R_{\Delta F}^{T'VA}$ responses would contain a factor $(q/m)^2$ and q/m , respectively, with respect to the $R_{\Delta F}^{TAA}$ coefficients. Therefore, if we define the coefficients

$$\tilde{C}'_{1,Vi} \equiv \frac{\tilde{C}_{1,Vi}}{(q/m_N)^2}, \quad \tilde{C}'_{1,VAi} \equiv \frac{\tilde{C}_{1,VAi}}{(q/m_N)}, \quad (102)$$

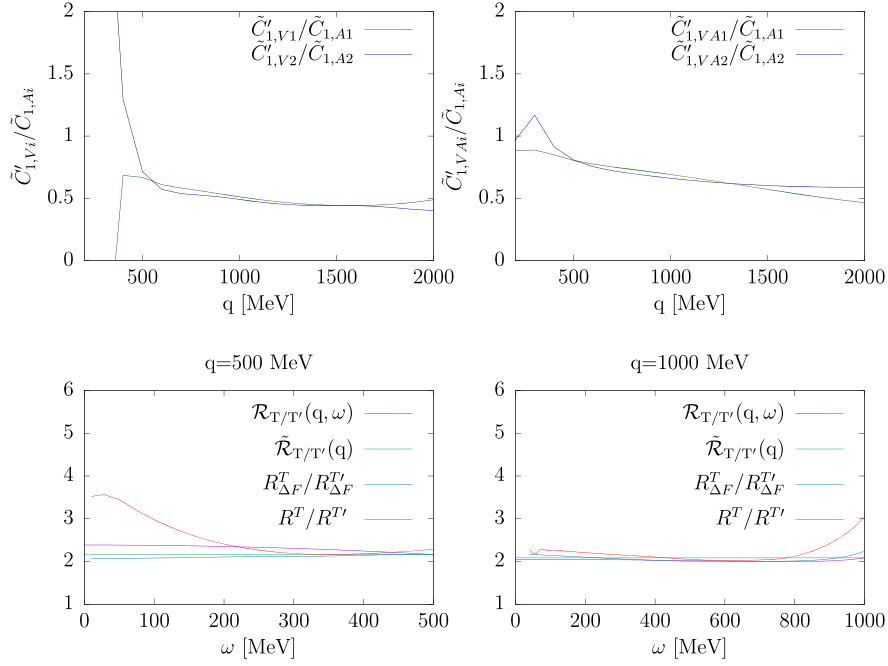


FIG. 9. Top: relation between the coefficients of the ΔF subresponses $R_{\Delta F}^{TVV}$ and $R_{\Delta F}^{TVA}$, with respect to $R_{\Delta F}^{TAA}$. Bottom: comparison of the quotient $R^T/R^{T'}$ with several approximations (see the text). The $\mathcal{R}_{T/T'}$ and $\tilde{\mathcal{R}}_{T/T'}$ functions have been obtained from the semiempirical formulas of the ΔF subresponses.

then one expects the quotients $\tilde{C}'_{1,Vi}/\tilde{C}_{1,Ai}$ and $\tilde{C}'_{1,VAi}/\tilde{C}_{1,Ai}$ to be approximately independent of q . This is shown in Fig. 9, in which we plot these quotients and see that they are roughly

$$\frac{\tilde{C}'_{1,Vi}}{\tilde{C}_{1,Ai}} \simeq \frac{1}{2} \quad (103)$$

$$\frac{\tilde{C}'_{1,VAi}}{\tilde{C}_{1,Ai}} \simeq \frac{1}{\sqrt{2}}. \quad (104)$$

If we neglect the small contributions of the SP and ΔB diagrams, the semiempirical formulas (66), (72), and (78) allow us to make quantitative estimations of relation between the T and T' responses. In fact, the following approximate formulas can be obtained between $R^{T,VV}$ and $R^{T,AA}$,

$$\frac{R^{T,AA}}{R^{T,VV}} \simeq \frac{R_{\Delta F}^{T,AA}}{R_{\Delta F}^{T,VV}} \simeq \frac{(C_5^A)^2}{(C_3^V)^2 \frac{1}{2} \left(\frac{q}{m_N}\right)^2}, \quad (105)$$

as can the following relation between the T and T' responses.

$$\begin{aligned} \frac{R^T}{R^{T'}} &\simeq \frac{R_{\Delta F}^T}{R_{\Delta F}^{T'}} \simeq \frac{(C_3^V)^2 \frac{1}{2} \left(\frac{q}{m_N}\right)^2 + (C_5^A)^2}{C_3^V C_5^A \frac{1}{\sqrt{2}} \left(\frac{q}{m_N}\right)} \\ &\equiv \mathcal{R}_{T/T'}(q, \omega), \end{aligned} \quad (106)$$

where we have defined the function $\mathcal{R}_{T/T'}(q, \omega)$ that represents the approximate quotient between the subresponses T and T' for the ΔF diagrams. To obtain Eq. (106), we have used the empirical relations (103) and (104) between the corresponding coefficients, and we have assumed that the averaged Δ propagators are similar for the VV , AA , and VA responses, and they cancel out in the numerator and denominator. The function \mathcal{R} depends on ω through the Q^2 dependence of the Δ form factors $C_3^V(Q^2)$ and $C_5^A(Q^2)$. The comparison between this relationship and the exact result is also shown in Fig. 9 for two values of the momentum transfer.

If we also assume that the form factors have an approximately similar dependence on Q^2 , and that this dependence is canceled in the numerator and the denominator, we can simply use the values at the origin, $Q^2 = 0$, of the form factors to obtain a simple approximate formula for the relationship between T and T' responses. In fact, inserting the values $C_5^A(0) = 1.2$, and $C_3^V(0) = 2.13$ in Eq. (106), we can write

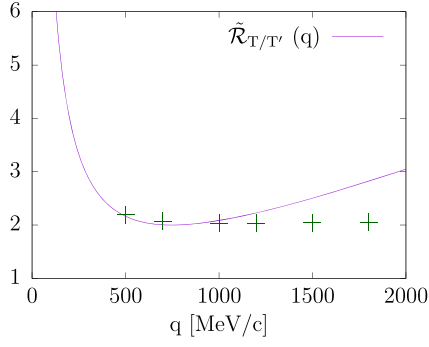


FIG. 10. The semiempirical approximation $\tilde{\mathcal{R}}_{T/T'}$ of the quotient between the T and T' responses, as a function of q .

$$\frac{R^T}{R^{T'}} \simeq \frac{(2.13)^2 \frac{1}{2} \left(\frac{q}{m_N}\right)^2 + (1.2)^2}{2.13 \times 1.2 \frac{1}{\sqrt{2}} \left(\frac{q}{m_N}\right)} \equiv \tilde{\mathcal{R}}_{T/T'}(q). \quad (107)$$

Note that this approximation does not depend on ω , and this relation is compared in Fig. 10 with the exact result computed for ω at the maximum of Δ peak. We see that the formula (107) is valid for q between 500 and 1100 MeV/c, where $\tilde{\mathcal{R}}_{T/T'} \simeq 2$. Note that this value depends on the value of C_A^5 , and here we have used 1.2.

For larger q , the approximations fail because in this region the dominance of the ΔF starts to decay.

Note that Eqs. (106) and (107) relate R^T and $R^{T'}$, similarly to Eqs. (8,9) of Ref. [19], but with the Δ form factors instead of the nucleon form factors, and with similar kinematic factors. In our case, we see, from Figs. 9 and 10, that this relationship is approximately $R^T \simeq 2R^{T'}$ in the region of the Δ peak. This opens the way to determine the 2p2h response of neutrinos from fits of the corresponding response in the electromagnetic channel.

Finally, in this work, we have considered the noninteracting free Δ in the MEC. The semiempirical formula can be extended to include the case of a Δ interacting with the mean field [56,72]. In this case, the Δ acquires effective mass, M_Δ^* , and vector energy, E_v^Δ (see Appendix A). In the simplest case of universal coupling, the Δ scalar and vector energies are the same as those of the nucleon. In Fig. 11, we show the effect of including the Δ self-energy for universal coupling, compared to the case of free Δ . In Fig. 11, we also compare with the extended semiempirical formula of Appendix A. The effect of the Δ interaction is a q -dependent shift, from -50 MeV, for small q , up to $+50$, for large q . The height of the transverse response decreases for low q by $\simeq 30\%$. The semiempirical formula allows us to easily study the dependence of the responses for other values of the Δ interaction with the mean field.

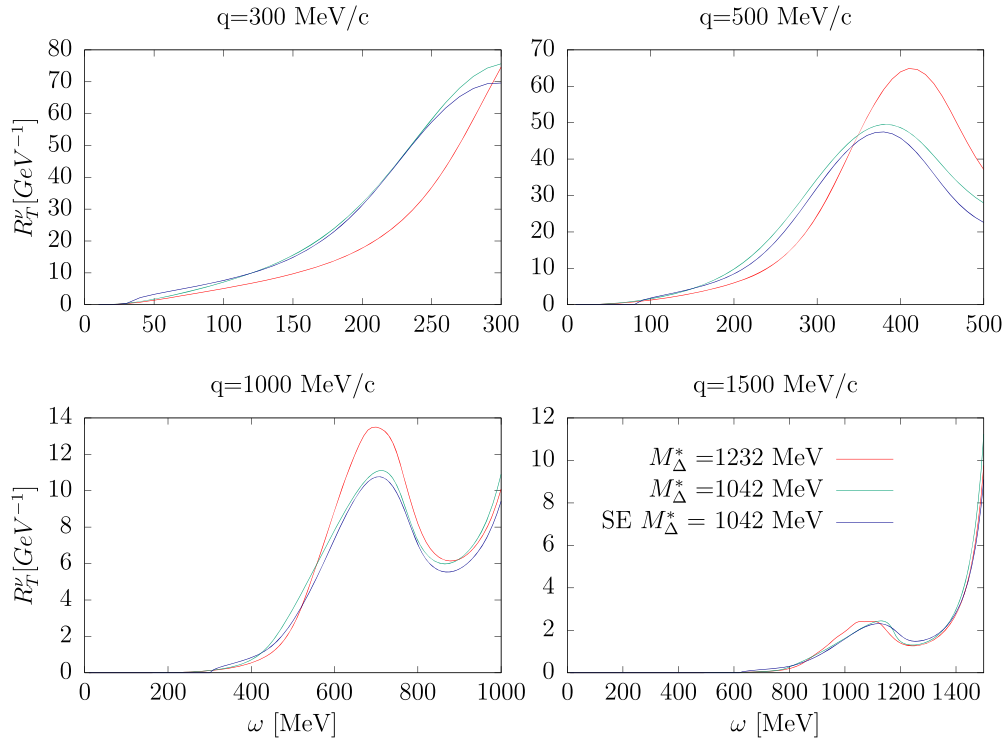


FIG. 11. Comparison of the transverse response functions including or not the Δ self-energy in the MEC, in the case of universal coupling, $E_v^\Delta = E_v$, and $M_\Delta^* = 1042$ MeV. The results of the modified semiempirical formula for interacting Δ are also shown.

V. CONCLUSIONS

In this article, we have proposed a semiempirical formula to approximately calculate the 2p2h responses in neutrino scattering. The formula is based on classifying the contribution of Feynman diagrams of MEC with a similar structure, in terms of the same electroweak form factor and the same number of delta-forward propagators, obtaining in our case six contributions, or subresponses, from our three types of diagrams: delta forward, seagull pionic, and delta backward.

It is proposed that each subresponse is the product of the phase-space function of two particles, electroweak form factors, and averaged delta propagators, multiplied by coefficients that only depend on q . These coefficients are fitted with a RMF model of nuclear matter for the 2p2h responses. In the SE formula, we use an approximation of the phase space (frozen nucleon approximation) and a model for the average propagator of the delta-forward current.

The hypothesis that the coefficients do not depend on ω is generally fulfilled, with two minor exceptions in the transverse SP subresponses, where a corrective term with a second-degree polynomial in ω is added. Altogether, we have shown that the dependence on ω of the 2p2h responses comes mainly from these three elements: phase space, form factor, and averaged propagator of the delta forward, and that is it.

Having extracted in the subresponses everything that can be factorized, the semiempirical formulas explicitly contain the dependence on the Fermi momentum, the number of particles, the effective mass and vector energy of the RMF, the electroweak form factors, and the coupling constants, in addition to the explicit dependence on q and ω through the phase space and the averaged Δ propagator.

The semiempirical formula has been obtained for free Δ , but then we have generalized it to include a Δ interacting with the mean field, which already depends on the Δ effective mass and its vector energy.

An advantage of the semiempirical formula is that it provides the 2p2h responses in a model in an easily reproducible way and that it also allows many of the model's parameters to be varied at will.

The semiempirical formula could be extended by including more diagrams or contributions to the MEC, for example, ρ -meson exchange, correlation diagrams, and excitation of other nucleon resonances, simply by adding the corresponding form factors, couplings, and propagators to construct the subresponses of the new contributions. The SE formula could also be fitted with other models to recalculate the coefficients.

The SE formulas are promising for application in neutrino calculations and event simulators because they are analytical and allow modifying physical parameters of the model. We are currently studying other nuclei, and we have checked that the formula is valid in symmetric nuclei,

$N = Z$, with the same coefficients of this article, and only the averaged Δ propagator must be modified by readjusting the effective width and shift.

In the future, we will apply the semiempirical formula to the case of asymmetric matter, $N \neq Z$, which is of interest for current and future neutrino experiments, since in this case the emission channels of pp, pn, and nn have to be treated separately.

ACKNOWLEDGMENTS

This work has been supported by the Spanish Agencia Estatal de investigacion (DOI 10.13039/501100011033, Grants No. FIS2017-85053-C2-1-P and No. PID2020-114767 GB-I00), the Junta de Andalucia (Grant No. FQM-225), and the European Regional Development Funds (Grant No. A-FQM-390-UGR20). V.L.M.-C. acknowledges a contract funded by Agencia Estatal de Investigacion and European Social Fund.

APPENDIX A: SEMIEMPIRICAL FORMULA FOR Δ IN THE MEDIUM

In this Appendix, we explain how the semiempirical formula must be modified to include the effective mass of the Δ and its vector energy. In this work, we have neglected the interaction of the Δ , treating it as a free particle. If we assume that the Δ interacts with the scalar and vector fields of the RMF, the Δ acquires an effective mass and a vector energy [56,72],

$$M_{\Delta}^* = M_{\Delta} - g_{\Delta}^{\Delta} \phi_0 \quad (\text{A1})$$

$$E_{\text{RMF}}^{\Delta} = E^{\Delta} + E_v^{\Delta} \quad (\text{A2})$$

with $E^{\Delta} = \sqrt{p_{\Delta}^2 + M_{\Delta}^{*2}}$ is the on-shell energy of the intermediate Δ isobar with momentum \mathbf{p}_{Δ} .

In this case, the delta current would be modified by substituting the propagator of the free delta, Eq. (45), for the propagator in the medium, which is the following [56]:

$$G_{\alpha\beta}(P) = \frac{\mathcal{P}_{\alpha\beta}(P^*)}{P^{*2} - M_{\Delta}^{*2} + iM_{\Delta}^* \Gamma_{\Delta}(P^{*2}) + \frac{\Gamma_{\Delta}(P^{*2})^2}{4}}. \quad (\text{A3})$$

The projector $\mathcal{P}_{\alpha\beta}(P^*)$ is now

$$\mathcal{P}_{\alpha\beta}(P^*) = -(P^* + M_{\Delta}^*) \times \left[g_{\alpha\beta} - \frac{1}{3} \gamma_{\alpha} \gamma_{\beta} - \frac{2P_{\alpha}^* P_{\beta}^*}{3 M_{\Delta}^{*2}} + \frac{1}{3} \frac{P_{\alpha}^* \gamma_{\beta} - P_{\beta}^* \gamma_{\alpha}}{M_{\Delta}^*} \right], \quad (\text{A4})$$

where $P^{*\mu} = P^{\mu} - \delta_{\mu,0} E_v^{\Delta}$. With the Δ in the medium, the peak position of the delta-forward response is expected at

$$\omega = \sqrt{q^2 + M_{\Delta}^{*2}} - m_N^* - E_v + E_v^{\Delta}. \quad (\text{A5})$$

In the particular case of a free Δ , we recover the original position of the peak at

$$\omega = \sqrt{q^2 + M_\Delta^2} - m_N^* - E_v. \quad (\text{A6})$$

We see that the position of the Δ -forward peak depends on q and the values of the vector energies and the effective masses. In this case, the averaged Δ propagator, Eq. (54), is still calculated with the same formula, but changing the values of the parameters a and b to include the vector energy and the effective mass of the Δ in the mean field

$$a \equiv m_N^{*2} + (\omega + E_v - E_v^\Delta)^2 - q^2 + 2m_N^*(\omega + E_v - E_v^\Delta + \Sigma) - M_\Delta^{*2} + \frac{\Gamma^2}{4} \quad (\text{A7})$$

$$b \equiv M_\Delta^* \Gamma. \quad (\text{A8})$$

Note that the Δ effective mass also appears in the numerator of the Δ propagator, and this modifies the values of the matrix elements of the delta-forward current operator and the values of the responses. We have computed the new responses. For simplicity, we have assumed universal coupling, where the scalar and vector self-energies of the Δ are the same as the nucleon, and also the case where only the vector energies are equal. For universal coupling, $E_v^\Delta = E_v = 141$ MeV, and $M_\Delta^* = 1042$ MeV. We have found that the semiempirical formula can be easily modified to include these cases in the following lines, by replacing the parameters of the Δ -forward responses

$$\tilde{C}_{1,ij} \rightarrow \left(\frac{M_\Delta^*}{M_\Delta}\right)^2 \tilde{C}_{1,ij} \quad (\text{A9})$$

$$\tilde{C}_{4,ij} \rightarrow \left(\frac{M_\Delta^*}{M_\Delta}\right) \tilde{C}_{4,ij} \quad (\text{A10})$$

$$\tilde{C}_{5,ij} \rightarrow \left(\frac{M_\Delta^*}{M_\Delta}\right) \tilde{C}_{5,ij}, \quad (\text{A11})$$

where $i = V, A, VA$, and $j = 1, 2$. The rest of the parameters of the SE formula are not modified.

APPENDIX B: TABLES OF COEFFICIENTS OF THE SEMIEMPIRICAL MEC FORMULAS

In this Appendix, we provide the values of the coefficients, $\tilde{C}_i(q)$, of the semiempirical MEC responses for $q = 200$ MeV/c up to $q = 2000$ MeV/c in steps of $\Delta q = 100$ MeV/c. These tables can be interpolated to compute them for other q values. Alternatively, polynomial parametrizations of these coefficient are provided in Appendix C. The tables are included as additional material in plain text [73].

In Table I, we give the averaged width, $\Gamma(q)$, and averaged shift, $\Sigma(q)$, of the averaged Δ propagator, $G_{\text{av}}(q, \omega)$, for each one of the response functions of the kind VV , AA , or VA .

The coefficients of the SE MEC are provided in Tables II (for the R_T^{VV} response function), III (for R_T^{AA}), IV (for R_{CC}^{VV}), V (for R_{CC}^{AA}), VI (for R_{CL}^{AA}), VII (for R_{LL}^{AA}), and VIII (for R_T^{VA}).

TABLE I. Values of the Σ and Γ parameters of the averaged Δ propagator in the vector, axial, and vector-axial responses.

q	Σ_V	Γ_V	Σ_A	Γ_A	Σ_{VA}	Γ_{VA}
200	429.56	411.88	370.98	354.59	-414.99	392.89
300	78.986	185.09	56.717	213.63	68.141	202.39
400	91.125	166.59	77.657	105.54	86.064	114.85
500	98.153	110.12	79.080	108.77	89.183	109.51
600	102.60	101.32	81.094	112.29	92.511	104.93
700	107.11	95.220	83.883	112.49	96.193	100.76
800	111.70	89.771	87.198	111.84	100.14	96.588
900	116.35	84.322	90.914	111.16	104.23	92.175
1000	120.93	79.042	94.968	110.81	108.29	87.599
1100	125.48	74.275	99.373	110.79	112.16	82.932
1200	130.43	70.570	104.18	110.83	115.85	78.412
1300	136.28	67.973	109.36	110.74	119.34	74.053
1400	143.48	66.060	114.90	110.19	122.58	69.760
1500	152.32	64.801	120.78	108.83	125.39	65.752
1600	163.36	63.297	126.84	106.84	127.73	61.963
1700	177.02	60.783	132.90	103.96	129.37	58.403
1800	193.85	56.980	138.53	100.53	130.07	55.603
1900	214.45	51.489	143.10	97.028	129.72	53.580
2000	239.30	44.367	145.85	94.244	128.13	52.692

TABLE II. Coefficients $\tilde{C}_i(q)$ of the R_T^{VV} response function in the semiempirical MEC formulas.

q	$\tilde{C}_{1,V1}$	$\tilde{C}_{1,V2}$	$\tilde{C}_{2,V}$	$\tilde{C}_{3,V}$	$\tilde{C}_{4,V1}$	$\tilde{C}_{4,V2}$	$\tilde{C}_{5,V1}$	$\tilde{C}_{5,V2}$	$\tilde{C}_{6,V}$
200	-5.6455	4.7254	324.95	0.8821	19.976	-11.856	-0.0750	-0.1005	4.9442
300	-2.3128	7.0572	277.05	1.6642	6.7713	-8.4869	-0.2942	-0.1056	8.2559
400	2.8522	5.6335	237.33	2.3559	-3.6706	-2.9271	-0.4448	-0.1328	10.339
500	4.6067	5.6932	207.99	2.9384	-4.6034	-2.4378	-0.4102	-0.2456	11.498
600	6.3810	7.3485	187.15	3.4589	-5.3142	-2.0497	-0.4561	-0.3564	12.148
700	8.6406	10.267	172.73	3.9693	-6.3515	-1.3441	-0.5438	-0.4778	12.560
800	11.229	14.080	163.24	4.5053	-7.4147	-0.2435	-0.6380	-0.5912	12.867
900	14.017	18.385	157.49	5.0833	-8.3548	1.2379	-0.7307	-0.6812	13.126
1000	16.967	22.966	154.81	5.7084	-9.1218	3.0420	-0.8307	-0.7465	13.364
1100	20.125	27.880	154.72	6.3784	-9.6915	5.1327	-0.9510	-0.7926	13.588
1200	23.578	33.383	156.96	7.0876	-10.030	7.5290	-1.1024	-0.8230	13.803
1300	27.448	39.763	161.41	7.8296	-10.104	10.278	-1.2937	-0.8428	14.007
1400	31.840	47.170	168.06	8.5967	-9.8987	13.412	-1.5289	-0.8607	14.200
1500	36.836	55.518	177.07	9.3820	-9.4335	16.925	-1.8104	-0.8945	14.380
1600	42.528	64.336	188.67	10.179	-8.7568	20.743	-2.1399	-0.9698	14.545
1700	49.031	72.952	203.28	10.980	-7.9275	24.742	-2.5173	-1.1085	14.696
1800	56.482	80.929	221.50	11.781	-6.9963	28.795	-2.9423	-1.3179	14.831
1900	65.053	88.622	244.16	12.577	-5.9638	32.999	-3.4146	-1.5896	14.948
2000	74.960	98.238	272.46	13.365	-4.7513	38.182	-3.9421	-2.0225	15.050

TABLE III. Coefficients $\tilde{C}_i(q)$ of the R_T^{AA} response function in the semiempirical MEC formulas.

q	$\tilde{C}_{1,A1}$	$\tilde{C}_{1,A2}$	$\tilde{C}_{2,A}$	$\tilde{C}_{3,A}$	$\tilde{C}_{4,A1}$	$\tilde{C}_{4,A2}$	$\tilde{C}_{5,A1}$	$\tilde{C}_{5,A2}$	$\tilde{C}_{6,A}$
200	16.329	34.206	19.944	20.615	4.1488	-2.5516	-2.7292	2.6273	17.649
300	21.430	18.820	18.724	18.470	3.7251	-0.2755	-2.3497	-0.0523	16.196
400	22.912	23.973	16.754	15.620	2.7107	1.3642	-2.1103	-1.1070	13.495
500	24.292	28.051	14.811	13.089	2.4231	1.8619	-2.2025	-1.5055	10.924
600	25.597	31.450	13.062	11.054	2.2471	2.2170	-2.3253	-1.7242	8.8130
700	26.669	34.336	11.520	9.4730	2.0649	2.5229	-2.3886	-1.8179	7.1491
800	27.590	36.844	10.172	8.2615	1.8603	2.7740	-2.3935	-1.8096	5.8390
900	28.405	39.083	8.9866	7.3289	1.6293	2.9601	-2.3566	-1.7396	4.7773
1000	29.015	41.136	7.9396	6.6055	1.3711	3.0905	-2.2927	-1.6460	3.8973
1100	29.845	43.044	7.0164	6.0317	1.0980	3.1824	-2.2107	-1.5499	3.1401
1200	30.530	44.799	6.1995	5.5604	0.8124	3.2402	-2.1127	-1.4694	2.4634
1300	31.210	46.400	5.4813	5.1521	0.5207	3.2635	-1.9980	-1.4097	1.8359
1400	31.879	47.821	4.8477	4.7766	0.2225	3.2622	-1.8677	-1.3610	1.2352
1500	32.511	49.056	4.2924	4.4065	-0.0743	3.2381	-1.7222	-1.3142	0.6426
1600	33.070	50.100	3.8069	4.0198	-0.3670	3.1950	-1.5655	-1.2580	0.0461
1700	33.514	50.979	3.3820	3.5983	-0.6496	3.1351	-1.4033	-1.1864	-0.5625
1800	33.803	51.770	3.0103	3.1267	-0.9176	3.0642	-1.2428	-1.1018	-1.1922
1900	33.905	52.613	2.6875	2.5931	-1.1712	2.9866	-1.0965	-0.9982	-1.8438
2000	33.778	53.762	2.4071	1.9874	-1.3992	2.9084	-0.9692	-0.8808	-2.5212

TABLE IV. Coefficients $\tilde{C}_i(q)$ of the R_{CC}^{VV} response function in the semiempirical MEC formulas.

q	$\tilde{C}_{1,V1}$	$\tilde{C}_{1,V2}$	$\tilde{C}_{2,V}$	$\tilde{C}_{3,V}$	$\tilde{C}_{4,V1}$	$\tilde{C}_{4,V2}$	$\tilde{C}_{5,V1}$	$\tilde{C}_{5,V2}$	$\tilde{C}_{6,V}$
200	-0.1024	0.0854	8.5525	0.0476	0.3211	-0.1617	0.0030	-0.0135	0.0357
300	-0.0486	0.1498	6.7440	0.1319	0.1593	-0.1606	-0.0159	-0.0211	0.1003
400	0.0678	0.1505	5.4143	0.2642	-0.0385	-0.0810	-0.0463	-0.0248	0.1893
500	0.1578	0.1882	4.5372	0.4452	-0.0496	-0.0868	-0.0653	-0.0422	0.3005
600	0.3027	0.2904	3.9966	0.6710	0.0294	-0.0948	-0.1020	-0.0694	0.4303
700	0.5658	0.4717	3.6898	0.9354	0.2210	-0.0787	-0.1666	-0.1106	0.5732
800	1.0273	0.7286	3.5402	1.2320	0.5934	-0.0121	-0.2661	-0.1706	0.7238
900	1.8174	1.0250	3.4920	1.5559	1.2182	0.1411	-0.4121	-0.2582	0.8770
1000	3.1690	1.2899	3.5088	1.9032	2.1686	0.4230	-0.6208	-0.3881	1.0291
1100	5.5066	1.4027	3.5654	2.2711	3.5213	0.8816	-0.9112	-0.5782	1.1773
1200	9.5630	1.1584	3.6453	2.6577	5.3523	1.5678	-1.3018	-0.8488	1.3193
1300	16.468	0.2226	3.7376	3.0612	7.7257	2.5367	-1.8108	-1.2243	1.4536
1400	27.710	-1.8853	3.8351	3.4808	10.692	3.8489	-2.4530	-1.7339	1.5790
1500	44.980	-5.7623	3.9328	3.9156	14.285	5.5617	-3.2416	-2.4152	1.6947
1600	70.073	-12.111	4.0275	4.3654	18.052	7.7114	-4.1882	-3.3012	1.8002
1700	104.98	-21.738	4.1169	4.8302	23.426	10.286	-5.3006	-4.4046	1.8959
1800	152.13	-35.588	4.1997	5.3101	29.007	13.208	-6.5868	-5.7040	1.9812
1900	214.67	-54.766	4.2747	5.8056	35.314	16.426	-8.0633	-7.1889	2.0576
2000	296.65	-80.395	4.3415	6.3170	42.457	20.217	-9.7724	-9.1248	2.1249

TABLE V. Coefficients $\tilde{C}_i(q)$ of the R_{CC}^{AA} response function in the semiempirical MEC formulas.

q	$\tilde{C}_{1,A1}$	$\tilde{C}_{1,A2}$	$\tilde{C}_{2,A1}$	$\tilde{C}_{2,A2}$	$\tilde{C}_{3,A}$	$\tilde{C}_{4,A1}$	$\tilde{C}_{4,A2}$	$\tilde{C}_{5,A1}$	$\tilde{C}_{5,A2}$	$\tilde{C}_{6,A}$
200	0.4310	0.6758	238.27	9.3999	0.3545	1.0876	-50.597	0.0504	-0.0292	0.3475
300	0.7425	0.6100	215.77	8.4094	0.3314	-8.2958	-11.926	0.0265	0.0090	0.0575
400	1.1073	1.3165	175.09	7.7175	0.3006	-7.1932	-8.0118	0.0064	0.0216	-0.1498
500	2.1427	2.1218	138.76	6.9936	0.2787	-4.9007	-7.7936	0.0210	0.0146	-0.3151
600	3.1362	3.1395	109.68	6.2763	0.2646	-0.4025	-8.1195	0.0515	0.0109	-0.4585
700	4.3281	4.3521	87.033	5.6002	0.2544	4.6146	-8.0345	0.0965	0.0144	-0.5908
800	5.7860	5.7550	69.523	4.9837	0.2442	10.156	-7.5209	0.1605	0.0296	-0.7057
900	7.6019	7.3393	55.929	4.4317	0.2305	16.577	-6.5162	0.2447	0.0588	-0.8128
1000	9.9183	9.1025	45.328	3.9429	0.2106	24.215	-4.9410	0.3495	0.1041	-0.9201
1100	12.958	11.016	37.025	3.5122	0.1822	33.432	-2.6731	0.4694	0.1641	-1.0171
1200	17.041	13.007	30.456	3.1346	0.1430	44.503	0.4040	0.5954	0.2368	-1.1184
1300	22.616	14.950	25.230	2.8037	0.0918	57.725	4.4288	0.7159	0.3149	-1.2640
1400	30.266	16.646	21.041	2.5137	0.0271	73.368	9.5238	0.8128	0.3868	-1.3986
1500	40.702	17.843	17.664	2.2593	-0.0514	91.621	15.780	0.8644	0.4368	-1.5547
1600	54.774	18.212	14.919	2.0359	-0.1444	112.59	23.235	0.8495	0.4422	-1.7426
1700	73.477	17.381	12.677	1.8392	-0.2522	136.52	31.950	0.7379	0.3723	-1.9275
1800	97.967	14.957	10.833	1.6658	-0.3739	163.50	41.932	0.5062	0.1975	-2.1423
1900	129.63	10.517	9.3095	1.5124	-0.5101	193.73	53.264	0.1143	-0.1323	-2.3821
2000	170.12	3.6516	8.0440	1.3765	-0.6595	227.56	66.185	-0.4731	-0.6773	-2.6522

TABLE VI. Coefficients $\tilde{C}_i(q)$ of the R_{CL}^{AA} response function in the semiempirical MEC formulas.

q	$\tilde{C}_{1,A1}$	$\tilde{C}_{1,A2}$	$\tilde{C}_{2,A1}$	$\tilde{C}_{2,A2}$	$\tilde{C}_{3,A}$	$\tilde{C}_{4,A1}$	$\tilde{C}_{4,A2}$	$\tilde{C}_{5,A1}$	$\tilde{C}_{5,A2}$	$\tilde{C}_{6,A}$
200	-1.1765	-2.5379	-72.678	-7.2538	0.0806	5.5173	34.373	0.0563	0.1300	-0.7486
300	-2.1851	-2.0364	-91.567	-7.3504	-0.1306	9.9664	13.202	0.1902	-0.0182	-0.6646
400	-3.0251	-3.6397	-86.641	-7.0749	-0.2579	8.1204	10.129	0.1989	0.0688	-0.4324
500	-4.9236	-5.0983	-75.322	-6.5790	-0.3193	6.9727	9.2048	0.1870	0.1269	-0.2418
600	-6.3387	-6.6909	-63.463	-5.9990	-0.3393	2.5570	9.3724	0.1727	0.1655	-0.1346
700	-7.8449	-8.3950	-52.859	-5.4096	-0.3340	-2.7198	9.1389	0.1527	0.1909	-0.1047
800	-9.5543	-10.225	-43.896	-4.8494	-0.3134	-8.5236	8.4471	0.1251	0.2045	-0.1183
900	-11.573	-12.190	-36.470	-4.3350	-0.2830	-15.121	7.2693	0.0907	0.2064	-0.1513
1000	-14.046	-14.312	-30.392	-3.8718	-0.2457	-22.835	5.5497	0.0531	0.2008	-0.1864
1100	-17.186	-16.579	-25.435	-3.4593	-0.2019	-32.018	3.1768	0.0182	0.1931	-0.2067
1200	-21.292	-18.932	-21.379	-3.0945	-0.1506	-42.966	0.0363	-0.0051	0.1917	-0.1904
1300	-26.782	-21.257	-18.053	-2.7730	-0.0910	-55.972	-4.0071	-0.0072	0.2058	-0.1377
1400	-34.193	-23.366	-15.321	-2.4898	-0.0212	-71.313	-9.0779	0.0268	0.2493	-0.0681
1500	-44.183	-25.025	-13.066	-2.2405	0.0598	-89.177	-15.266	0.1140	0.3370	0.0141
1600	-57.540	-25.924	-11.196	-2.0209	0.1528	-109.72	-22.625	0.2718	0.4888	0.1558
1700	-75.203	-25.715	-9.6367	-1.8273	0.2584	-133.11	-31.192	0.5271	0.7308	0.3566
1800	-98.277	-24.042	-8.3357	-1.6560	0.3769	-159.48	-40.991	0.9038	1.0907	0.5645
1900	-128.11	-20.522	-7.2402	-1.5045	0.5089	-189.04	-52.100	1.4318	1.6084	0.8363
2000	-166.30	-14.797	-6.3199	-1.3699	0.6537	-222.20	-64.787	2.1540	2.3542	1.1126

TABLE VII. Coefficients $\tilde{C}_i(q)$ of the R_{LL}^{AA} response function in the semiempirical MEC formulas.

q	$\tilde{C}_{1,A1}$	$\tilde{C}_{1,A2}$	$\tilde{C}_{2,A1}$	$\tilde{C}_{2,A2}$	$\tilde{C}_{3,A}$	$\tilde{C}_{4,A1}$	$\tilde{C}_{4,A2}$	$\tilde{C}_{5,A1}$	$\tilde{C}_{5,A2}$	$\tilde{C}_{6,A}$
200	7.7088	17.531	233.20	5.0374	9.4317	3.1687	-49.648	-1.2839	1.2848	3.4218
300	10.129	9.2250	180.29	6.0908	8.1410	-5.1516	-17.177	-1.1784	0.1189	2.1615
400	10.742	11.672	130.90	6.3740	6.7068	-5.1196	-11.029	-0.9983	-0.4267	1.5098
500	12.296	13.556	95.868	6.1594	5.5049	-5.8216	-8.7191	-0.9352	-0.6065	1.2160
600	13.590	15.271	71.787	5.7313	4.5619	-2.0130	-8.5029	-0.8949	-0.6911	1.1226
700	14.933	16.968	55.051	5.2304	3.8319	3.0303	-8.0879	-0.8569	-0.7349	1.1446
800	16.477	18.749	43.149	4.7251	3.2680	8.6441	-7.2951	-0.8243	-0.7630	1.2170
900	18.343	20.667	34.439	4.2463	2.8272	15.023	-6.0701	-0.8030	-0.7775	1.3022
1000	20.673	22.776	27.928	3.8069	2.4761	22.503	-4.3435	-0.8019	-0.7903	1.3936
1100	23.665	25.080	22.940	3.4113	2.1877	31.380	-2.0133	-0.8286	-0.8101	1.4126
1200	27.589	27.524	19.060	3.0580	1.9416	42.013	1.0546	-0.8948	-0.8527	1.4160
1300	32.827	29.998	15.983	2.7448	1.7231	54.657	4.9885	-1.0084	-0.9300	1.3692
1400	39.872	32.313	13.511	2.4679	1.5207	69.579	9.9124	-1.1826	-1.0605	1.2548
1500	49.320	34.251	11.500	2.2234	1.3272	86.942	15.909	-1.4322	-1.2638	1.0643
1600	61.902	35.509	9.8547	2.0074	1.1366	106.95	23.046	-1.7716	-1.5598	0.8203
1700	78.500	35.763	8.4949	1.8163	0.9445	129.79	31.376	-2.2227	-1.9720	0.5642
1800	100.17	34.688	7.3611	1.6472	0.7488	155.55	40.907	-2.8139	-2.5330	0.2057
1900	128.23	31.939	6.4108	1.4973	0.5476	184.45	51.726	-3.5732	-3.2833	-0.2214
2000	164.22	27.217	5.6116	1.3640	0.3392	216.84	64.070	-4.5204	-4.2713	-0.6653

TABLE VIII. Coefficients $\tilde{C}_i(q)$ of the R_T^{VA} response function in the semiempirical MEC formulas.

q	$\tilde{C}_{1,VA1}$	$\tilde{C}_{1,VA2}$	$\tilde{C}_{2,VA}$	$\tilde{C}_{3,VA}$	$\tilde{C}_{4,VA1}$	$\tilde{C}_{4,VA2}$	$\tilde{C}_{5,VA1}$	$\tilde{C}_{5,VA2}$	$\tilde{C}_{6,VA}$	$\tilde{C}_{6,AV}$
200	3.0775	7.0669	33.839	4.1248	-122.58	175.36	-0.28107	0.16341	-84.995	135.39
300	6.0856	7.0257	39.591	5.2873	-45.017	68.720	-0.36476	-0.00935	-5.9848	24.604
400	8.2977	9.3332	40.713	5.6595	10.642	-13.723	-0.41794	-0.17344	6.0440	6.4537
500	10.413	12.083	39.821	5.6071	20.192	-31.555	-0.44973	-0.30008	5.8446	5.3355
600	12.682	15.166	38.151	5.3665	17.331	-30.514	-0.49020	-0.39654	4.1826	6.3500
700	14.967	18.484	36.245	5.0677	12.947	-26.221	-0.52323	-0.46538	2.9376	6.8790
800	17.214	21.943	34.390	4.7752	9.2326	-22.152	-0.53893	-0.50361	2.1534	6.8773
900	19.389	25.464	32.660	4.5129	6.4570	-19.001	-0.53699	-0.51340	1.6290	6.6367
1000	21.465	29.016	31.110	4.2871	4.4528	-16.072	-0.51836	-0.49662	1.2863	6.2528
1100	23.421	32.597	29.762	4.0941	3.0130	-15.132	-0.48558	-0.45727	1.0445	5.8248
1200	25.233	36.210	28.602	3.9272	1.9657	-14.031	-0.44114	-0.39951	0.86212	5.3968
1300	26.891	39.863	27.639	3.7794	1.1886	-13.267	-0.38738	-0.32521	0.71212	4.9943
1400	28.388	43.548	26.853	3.6443	0.59663	-12.723	-0.32579	-0.23678	0.59011	4.6091
1500	29.714	47.274	26.240	3.5167	0.13074	-12.320	-0.25785	-0.13292	0.48717	4.2444
1600	30.863	51.023	25.787	3.3926	-0.24908	-12.001	-0.18497	-0.01558	0.39962	3.8983
1700	31.828	54.804	25.479	3.2691	-0.57026	-11.726	-0.10735	0.11481	0.32699	3.5639
1800	32.598	58.687	25.307	3.1443	-0.85053	-11.474	-0.02521	0.25836	0.26413	3.2461
1900	33.166	62.755	25.264	3.0170	-1.1045	-11.225	0.06088	0.41597	0.21063	2.9409
2000	33.523	67.137	25.330	2.8868	-1.3401	-10.971	0.15142	0.59231	0.16352	2.6510

APPENDIX C: PARAMETRIZATIONS OF NUCLEAR RESPONSE COEFFICIENTS

In this Appendix, we provide parametrizations of the q dependence of the semiempirical formula coefficients, $\tilde{C}_i(q)$, and of the averaged width, $\Gamma(q)$, and averaged shift, $\Sigma(q)$, of the averaged Δ propagator, $G_{av}(q, \omega)$, for each one of the response functions in the semiempirical MEC formulas. We provide two kind of parametrizations. Most of the coefficients allow a polynomial parametrization,

$$\tilde{C}_i(q) = \sum_{j=0}^8 a_j \left(\frac{q}{2m_N} \right)^j, \quad (\text{C1})$$

where the maximum range of the polynomial is 8 for some of the coefficients, but in many cases, the polynomial

degree is less or much less than 8. The factors in the polynomial are dimensionless.

For some of the coefficients, the parametrization is better written as a polynomial of the inverse variable $2m_N/q$,

$$\tilde{C}_i(q) = \sum_{j=0}^8 a_j \left(\frac{2m_N}{q} \right)^j. \quad (\text{C2})$$

These are labeled with a star symbol (*) in the tables below.

The parameters of the averaged width, $\Gamma(q)$, and averaged shift, $\Sigma(q)$, are given in Table IX.

Parameters are provided in Tables X (for the R_T^{VV} response function), XI (for R_T^{AA}), XII (for R_{CC}^{VV}), XIII (for R_{CC}^{AA}), XIV (for R_{CL}^{AA}), XV (for R_{LL}^{AA}), and XVI (for R_T^{VA}).

TABLE IX. Parameters of the effective shift, Σ , and width, Γ , of the averaged Δ propagator in the vector, axial, and vector-axial responses in the polynomial interpolations given by Eq. (C1), or Eq. (C2) for the ones labeled with a star symbol *.

	a_0	a_1	a_2	a_3	a_4	a_5	a_6
Σ_V	60.5191	174.869	-142.624	0.0	64.8675	51.5966	0.0
Γ_V	1450.93	-14248.6	60480.2	-132124	155882	-94328.1	22938.6
Σ_A^*	93.7987	-207.022	880.16	-1497.82	1345.81	-472.81	0.0
Γ_A	48.5674	457.116	-983.684	0.0	2539.27	-3068.47	1104.8
Σ_{VA}^*	83.6648	-43.5277	349.139	-500.553	371.11	-129.884	0.0
Γ_{VA}^*	173.605	-566.125	2174.47	-4916.66	5945.42	-3691.91	935.097

TABLE X. Parameters of the coefficients $\tilde{C}_i(q)$ of the response function R_T^{VV} in the interpolations given by Eq. (C1), or Eq. (C2) for the ones labeled with a star symbol *.

	a_0	a_1	a_2	a_3	a_4	a_5	a_6	a_7	a_8
$\tilde{C}_{1,V1}$	-19.6664	174.729	-504.898	878.162	-695.892	230.403	0.0	0.0	0.0
$\tilde{C}_{1,V2}$	0.0	253.264	-2441.02	9243.9	-14669.3	5825.93	10974.9	-13547.1	4446.27
$\tilde{C}_{2,V}$	464.634	-1606.42	3069.48	-2681.38	991.981	0.0	0.0	0.0	0.0
$\tilde{C}_{3,V}$	0.0	10.3393	0.0	2.04851	0.0	0.0	0.0	0.0	0.0
$\tilde{C}_{4,V1}$	94.6881	-1119.14	5033.78	-11612.8	14309.6	-8943.98	2231.48	0.0	0.0
$\tilde{C}_{4,V2}$	-32.638	281.151	-1007.61	1735.12	-1334.5	390.521	0.0	0.0	0.0
$\tilde{C}_{5,V1}$	0.0	-2.28139	4.09607	-5.10766	0.0	0.0	0.0	0.0	0.0
$\tilde{C}_{5,V2}$	0.0	0.0	-4.75457	0.0	12.9405	-9.69383	0.0	0.0	0.0
$\tilde{C}_{6,V}$	-8.6321	188.024	-702.668	1404.74	-1543.33	882.04	-205.234	0.0	0.0

TABLE XI. Parameters of the coefficients $\tilde{C}_i(q)$ of the response function R_T^{AA} in the polynomial interpolations given by Eq. (C1), or Eq. (C2) for the ones labeled with a star symbol *.

	a_0	a_1	a_2	a_3	a_4	a_5	a_6
$\tilde{C}_{1,A1}^*$	40.1435	-6.64283	0.0	0.354216	-0.0596866	0.00286741	0.0
$\tilde{C}_{1,A2}^*$	70.1364	-18.7631	0.0	1.64276	-0.448886	0.0478086	-0.0017799
$\tilde{C}_{2,A}^*$	-4.81568	8.57371	-1.05139	0.0446577	0.0	0.0	0.0
$\tilde{C}_{3,A}^*$	-1.70277	4.96453	-0.275884	0.0	0.0	0.0	0.0
$\tilde{C}_{4,A1}^*$	-7.1971	8.61063	-2.84088	0.399384	-0.0192562	0.0	0.0
$\tilde{C}_{4,A2}^*$	2.41265	1.1986	-0.572642	0.0682446	-0.00286093	0.0	0.0
$\tilde{C}_{5,A1}^*$	3.60383	-7.63457	3.56018	-0.757029	0.0746929	-0.00277361	0.0
$\tilde{C}_{5,A2}^*$	0.564127	-2.1691	0.636593	-0.0652588	0.00261604	0.0	0.0
$\tilde{C}_{6,A}^*$	-6.78958	6.19498	-0.386024	0.0	0.0	0.0	0.0

TABLE XII. Parameters of the coefficients $\tilde{C}_i(q)$ of the response function R_{CC}^{VV} in the polynomial interpolations given by Eq. (C1), or Eq. (C2) for the ones labeled with a star symbol *.

	a_0	a_1	a_2	a_3	a_4	a_5	a_6	a_7	a_8
$\tilde{C}_{1,V1}$	5.86212	-159.987	1683.15	-9120.25	28225.1	-51256.7	53538.9	-29301.5	6584.11
$\tilde{C}_{1,V2}$	0.0	10.2676	-141.292	839.978	-2670.46	4936.0	-5039.63	2519.75	-504.43
$\tilde{C}_{2,V}$	13.7234	-61.873	132.704	-119.937	39.5931	0.0	0.0	0.0	0.0
$\tilde{C}_{3,V}$	-0.0686547	0.0	8.18253	-2.41841	0.0	0.0	0.0	0.0	0.0
$\tilde{C}_{4,V1}$	1.75335	-23.1728	127.716	-386.742	628.412	-421.798	107.647	0.0	0.0
$\tilde{C}_{4,V2}$	0.0	-4.25877	36.7999	-123.11	166.971	-60.689	0.0	0.0	0.0
$\tilde{C}_{5,V1}$	0.0	-1.50012	8.60699	-14.8142	0.0	0.0	0.0	0.0	0.0
$\tilde{C}_{5,V2}$	0.0	0.542587	-6.74484	22.0466	-29.4463	6.74147	0.0	0.0	0.0
$\tilde{C}_{6,V}$	0.0	-0.288279	5.91647	0.0	-10.6428	9.91934	-2.86346	0.0	0.0

TABLE XIII. Parameters of the coefficients $\tilde{C}_i(q)$ of the response function R_{CC}^{AA} in the polynomial interpolations given by Eq. (C1), or Eq. (C2) for the ones labeled with a star symbol *.

	a_0	a_1	a_2	a_3	a_4	a_5	a_6
$\tilde{C}_{1,A1}$	1.00967	-13.0344	73.0221	0.0	-198.704	259.352	0.0
$\tilde{C}_{1,A2}$	3.83926	-62.2338	400.672	-1071.58	1612.63	-1160.11	288.513
$\tilde{C}_{2,A1}^*$	-39.489	44.8644	1.70487	-0.355919	0.0	0.0	0.0
$\tilde{C}_{2,A2}^*$	-2.17605	4.26239	-0.589857	0.0284662	0.0	0.0	0.0
$\tilde{C}_{3,A}$	0.491785	-1.6485	4.50652	-5.29804	1.47136	0.0	0.0
$\tilde{C}_{4,A1}$	0.0	-39.1279	69.8619	155.687	0.0	0.0	0.0
$\tilde{C}_{4,A2}$	-237.745	3006.35	-14949.7	36613.0	-47206.4	30846.5	-8019.86
$\tilde{C}_{5,A1}$	0.0888813	-0.283259	-1.87097	7.84059	0.0	-5.55097	0.0
$\tilde{C}_{5,A2}$	-0.408277	5.44882	-22.9732	37.91	-20.0388	0.0	0.0
$\tilde{C}_{6,A}$	1.04713	-8.02409	14.0568	-12.9651	3.55436	0.0	0.0

TABLE XIV. Parameters of the coefficients $\tilde{C}_i(q)$ of the response function R_{CL}^{AA} in the polynomial interpolations given by Eq. (C1), or Eq. (C2) for the ones labeled with a star symbol *.

	a_0	a_1	a_2	a_3	a_4	a_5	a_6
$\tilde{C}_{1,A1}$	0.0	-5.53339	-53.5517	0.0	177.554	-239.114	0.0
$\tilde{C}_{1,A2}$	-9.61627	139.949	-899.062	2402.54	-3417.33	2375.71	-613.648
$\tilde{C}_{2,A1}^*$	0.0	11.7941	-25.2288	6.74752	-0.71334	0.0274023	0.0
$\tilde{C}_{2,A2}^*$	2.15609	-4.27799	0.628945	-0.0298366	0.0	0.0	0.0
$\tilde{C}_{3,A}$	0.636771	-7.06185	17.1626	-16.5615	6.28956	0.0	0.0
$\tilde{C}_{4,A1}$	0.0	56.6646	-111.747	-126.814	0.0	0.0	0.0
$\tilde{C}_{4,A2}$	136.9	-1630.92	7986.45	-19326.8	24651.6	-16013.6	4146.06
$\tilde{C}_{5,A1}$	0.0	1.19682	-1.25693	-2.63388	0.0	3.99421	0.0
$\tilde{C}_{5,A2}$	0.325959	-3.9354	18.934	-32.2136	18.3759	0.0	0.0
$\tilde{C}_{6,A}$	-1.6945	10.4321	-24.2097	21.6826	-5.45423	0.0	0.0

TABLE XV. Parameters of the coefficients $\tilde{C}_i(q)$ of the response function R_{LL}^{AA} in the polynomial interpolations given by Eq. (C1), or Eq. (C2) for the ones labeled with a star symbol *.

	a_0	a_1	a_2	a_3	a_4	a_5	a_6	a_7	a_8
$\tilde{C}_{1,A1}$	6.14051	16.8939	26.5549	0.0	-131.934	203.693	0.0	0.0	0.0
$\tilde{C}_{1,A2}$	141.573	-2569.7	19929.8	-81032.4	193118	-278723	239909	-113349	22609.3
$\tilde{C}_{2,A1}^*$	-12.4591	12.5106	6.0512	-0.490028	0.0	0.0	0.0	0.0	0.0
$\tilde{C}_{2,A2}^*$	-2.2448	4.431	-0.710191	0.0341804	0.0	0.0	0.0	0.0	0.0
$\tilde{C}_{3,A}$	13.7017	-45.4469	66.7382	-45.3372	10.9484	0.0	0.0	0.0	0.0
$\tilde{C}_{4,A1}$	0.0	-34.6322	55.3018	156.919	0.0	0.0	0.0	0.0	0.0
$\tilde{C}_{4,A2}$	-204.783	2442.11	-11760.5	28204.8	-35811.5	23149.8	-5969.69	0.0	0.0
$\tilde{C}_{5,A1}$	-1.63891	4.02606	-6.87094	5.50556	0.0	-4.39721	0.0	0.0	0.0
$\tilde{C}_{5,A2}$	3.52402	-29.492	67.8688	-60.0326	14.9714	0.0	0.0	0.0	0.0
$\tilde{C}_{6,A}$	6.74744	-43.2203	113.243	-117.526	40.5894	0.0	0.0	0.0	0.0

TABLE XVI. Parameters of the coefficients $\tilde{C}_i(q)$ of the response function R_T^{VA} in the polynomial interpolations given by Eq. (C1), or Eq. (C2) for the ones labeled with a star symbol *.

	a_0	a_1	a_2	a_3	a_4	a_5	a_6	a_7	a_8
$\tilde{C}_{1,VA1}$	-12.5654	271.856	-1772.34	7170.88	-16850.5	23866.6	-20160.5	9354.45	-1834.88
$\tilde{C}_{1,VA2}$	25.7693	-401.628	3111.18	-11803.4	27278.8	-38962.8	33541.9	-15937.6	3209.45
$\tilde{C}_{2,VA}$	0.981663	516.73	-2461.18	5506.71	-6578.11	4042.59	-1002.31	0.0	0.0
$\tilde{C}_{3,VA}$	-0.698901	70.138	-272.492	456.781	-355.974	105.235	0.0	0.0	0.0
$\tilde{C}_{4,VA1}^*$	-12.6139	27.5451	-27.9095	15.1272	-3.53758	0.346934	-0.0120447	0.0	0.0
$\tilde{C}_{4,VA2}^*$	-21.627	21.438	-11.7492	0.0	0.549239	-0.0443672	0.0	0.0	0.0
$\tilde{C}_{5,VA1}$	-0.239117	0.0	-6.79621	17.8376	-15.5393	4.77589	0.0	0.0	0.0
$\tilde{C}_{5,VA2}$	0.570313	-3.93619	0.0	12.945	-14.1847	4.9816	0.0	0.0	0.0
$\tilde{C}_{6,VA}^*$	-3.54219	8.09376	-6.67611	2.807	-0.500736	0.035343	-0.000846361	0.0	0.0
$\tilde{C}_{6,AV}^*$	-0.47772	0.0	6.24771	-3.31642	0.616557	-0.0426815	0.000953283	0.0	0.0

- [1] H. Gallagher, G. Garvey, and G. P. Zeller, *Annu. Rev. Nucl. Part. Sci.* **61**, 355 (2011).
- [2] J. G. Morfin, J. Nieves, and J. T. Sobczyk, *Adv. High Energy Phys.* **2012**, 35 (2012).
- [3] J. A. Formaggio and G. P. Zeller, *Rev. Mod. Phys.* **84**, 1307 (2012).
- [4] L. Alvarez-Ruso, Y. Hayato, and J. Nieves, *New J. Phys.* **16**, 075015 (2014).
- [5] U. Mosel, *Annu. Rev. Nucl. Part. Sci.* **66**, 171 (2016).
- [6] A. M. Ankowski and C. Mariani, *J. Phys. G* **44**, 054001 (2017).
- [7] O. Benhar, P. Huber, C. Mariani, and D. Meloni, *Phys. Rep.* **700**, 1 (2017).
- [8] T. Katori and M. Martini, *J. Phys. G* **45**, 013001 (2018).
- [9] J. E. Amaro, M. B. Barbaro, J. A. Caballero, R. González-Jiménez, G. D. Megias, and I. Ruiz Simo, *J. Phys. G* **47**, 124001 (2020).
- [10] V Lyubushkin *et al.* (NOMAD Collaboration), *Eur. Phys. J. C* **63**, 355 (2009).
- [11] A. Aguilar-Arevalo *et al.* (MiniBooNE Collaboration), *Phys. Rev. D* **81**, 092005 (2010).
- [12] A. Aguilar-Arevalo *et al.* (MiniBooNE Collaboration), *Phys. Rev. D* **88**, 032001 (2013).
- [13] G. A. Fiorentini *et al.* (MINERvA Collaboration), *Phys. Rev. Lett.* **111**, 022502 (2013).
- [14] K. Abe *et al.* (T2K Collaboration), *Phys. Rev. D* **87**, 092003 (2013).
- [15] K. Abe *et al.* (T2K Collaboration), *Phys. Rev. D* **93**, 112012 (2016).
- [16] K. Abe *et al.* (T2K Collaboration), *Phys. Rev. D* **97**, 012001 (2018).
- [17] M. Martini, M. Ericson, G. Chanfray, and J. Marteau, *Phys. Rev. C* **80**, 065501 (2009).
- [18] J. Nieves, I. Ruiz Simo, and M. J. Vicente Vacas, *Phys. Rev. C* **83**, 045501 (2011).
- [19] K. Gallmeister, U. Mosel, and J. Weil, *Phys. Rev. C* **94**, 035502 (2016).
- [20] G. D. Megias, J. E. Amaro, M. B. Barbaro, J. A. Caballero, T. W. Donnelly, and I. Ruiz Simo, *Phys. Rev. D* **94**, 093004 (2016).
- [21] G. D. Megias, M. V. Ivanov, R. Gonzalez-Jimenez, M. B. Barbaro, J. A. Caballero, T. W. Donnelly, and J. M. Udias, *Phys. Rev. D* **89**, 093002 (2014); **91**, 039903(E) (2015).
- [22] A. M. Ankowski, *Phys. Rev. D* **92**, 013007 (2015).
- [23] R. Gran, J. Nieves, F. Sanchez, and M. J. Vicente Vacas, *Phys. Rev. D* **88**, 113007 (2013).
- [24] V. Pandey, N. Jachowicz, M. Martini, R. Gonzalez-Jimenez, J. Ryckebusch, T. Van Cuyck, and N. Van Dessel, *Phys. Rev. C* **94**, 054609 (2016).
- [25] M. Martini, N. Jachowicz, M. Ericson, V. Pandey, T. Van Cuyck, and N. Van Dessel, *Phys. Rev. C* **94**, 015501 (2016).
- [26] A. Lovato, S. Gandolfi, J. Carlson, Steven C. Pieper, and R. Schiavilla, *Phys. Rev. Lett.* **117**, 082501 (2016).
- [27] V. Pandey, N. Jachowicz, T. Van Cuyck, J. Ryckebusch, and M. Martini, *Phys. Rev. C* **92**, 024606 (2015).
- [28] A. M. Ankowski, O. Benhar, and M. Sakuda, *Phys. Rev. D* **91**, 033005 (2015).
- [29] N. Rocco, A. Lovato, and O. Benhar, *Phys. Rev. Lett.* **116**, 192501 (2016).
- [30] J. E. Amaro, M. B. Barbaro, J. A. Caballero, T. W. Donnelly, and A. Molinari, *Phys. Rep.* **368**, 317 (2002).
- [31] J. E. Amaro, M. B. Barbaro, J. A. Caballero, T. W. Donnelly, and C. Maieron, *Phys. Rev. C* **71**, 065501 (2005).
- [32] J. A. Caballero, J. E. Amaro, M. B. Barbaro, T. W. Donnelly, and J. M. Udias, *Phys. Lett. B* **653**, 366 (2007).
- [33] J. M. Udias, J. A. Caballero, E. Moya de Guerra, J. E. Amaro, and T. W. Donnelly, *Phys. Rev. Lett.* **83**, 5451 (1999).
- [34] A. Bodek, M. E. Christy, and B. Coopersmith, *Eur. Phys. J. C* **74**, 3091 (2014).
- [35] J. E. Sobczyk, *Phys. Rev. C* **96**, 045501 (2017).
- [36] M. Martini, M. Ericson, G. Chanfray, and J. Marteau, *Phys. Rev. C* **81**, 045502 (2010).

- [37] J. E. Amaro, M. B. Barbaro, J. A. Caballero, T. W. Donnelly, and C. F. Williamson, *Phys. Lett. B* **696**, 151 (2011).
- [38] J. E. Amaro, M. B. Barbaro, J. A. Caballero, and T. W. Donnelly, *Phys. Rev. Lett.* **108**, 152501 (2012).
- [39] J. Nieves, I. Ruiz Simo, and M. J. Vicente Vacas, *Phys. Lett. B* **707**, 72 (2012).
- [40] J. Nieves, I. Ruiz Simo, and M. J. Vicente Vacas, *Phys. Lett. B* **721**, 90 (2013).
- [41] I. Ruiz Simo, J. E. Amaro, M. B. Barbaro, J. A. Caballero, G. D. Megias, and T. W. Donnelly, *Phys. Lett. B* **770**, 193 (2017).
- [42] I. Ruiz Simo, J. E. Amaro, M. B. Barbaro, J. A. Caballero, G. D. Megias, and T. W. Donnelly, *Ann. Phys. (Amsterdam)* **388**, 323 (2018).
- [43] J. E. Sobczyk, J. Nieves, and F. Sánchez, *Phys. Rev. C* **102**, 024601 (2020).
- [44] S. Dolan, G. D. Megias, and S. Bolognesi, *Phys. Rev. D* **101**, 033003 (2020).
- [45] O. Lalakulich, K. Gallmeister, and U. Mosel, *Phys. Rev. C* **86**, 014614 (2012); **90**, 029902(E) (2014).
- [46] G. D. Megias, T. W. Donnelly, O. Moreno, C. F. Williamson, J. A. Caballero, R. González-Jiménez, A. De Pace, M. B. Barbaro, W. M. Alberico, M. Nardi, and J. E. Amaro, *Phys. Rev. D* **91**, 073004 (2015).
- [47] C. F. von Weizsäcker, *Z. Phys. A Hadrons Nucl.* **96**, 431 (1935).
- [48] J. E. Amaro, E. Ruiz Arriola, and I. Ruiz Simo, *Phys. Rev. C* **92**, 054607 (2015).
- [49] J. E. Amaro, E. Ruiz Arriola, and I. Ruiz Simo, *Phys. Rev. D* **95**, 076009 (2017).
- [50] V. L. Martínez-Consentino, I. Ruiz Simo, J. E. Amaro, and E. Ruiz Arriola, *Phys. Rev. C* **96**, 064612 (2017).
- [51] I. Ruiz Simo, V. L. Martínez-Consentino, J. E. Amaro, and E. Ruiz Arriola, *Phys. Rev. D* **97**, 116006 (2018).
- [52] J. E. Amaro, V. L. Martínez-Consentino, E. Ruiz Arriola, and I. Ruiz Simo, *Phys. Rev. C* **98**, 024627 (2018).
- [53] V. L. Martínez-Consentino, I. R. Simo, and J. E. Amaro, *Phys. Rev. C* **104**, 025501 (2021).
- [54] R. Rosenfelder, *Ann. Phys. (N.Y.)* **128**, 188 (1980).
- [55] B. D. Serot and J. D. Walecka, in *Advances in Nuclear Physics*, edited by J. W. Negele and E. Vogt (Plenum, New York, 1986), Vol. 16.
- [56] K. Wehrberger, *Phys. Rep.* **225**, 273 (1993).
- [57] M. B. Barbaro, R. Cenni, A. De Pace, T. W. Donnelly, and A. Molinari, *Nucl. Phys. A* **643**, 137 (1998).
- [58] I. Ruiz Simo, C. Albertus, J. E. Amaro, M. B. Barbaro, J. A. Caballero, and T. W. Donnelly, *Phys. Rev. D* **90**, 033012 (2014).
- [59] E. Hernandez, J. Nieves, and M. Valverde, *Phys. Rev. D* **76**, 033005 (2007).
- [60] J. E. Amaro, C. Maieron, M. B. Barbaro, J. A. Caballero, and T. W. Donnelly, *Phys. Rev. C* **82**, 044601 (2010).
- [61] T. Van Cuyck, N. Jachowicz, R. González-Jiménez, M. Martini, V. Pandey, J. Ryckebusch, and N. Van Dessel, *Phys. Rev. C* **94**, 024611 (2016).
- [62] B. Sommer, *Nucl. Phys. A* **308**, 263 (1978).
- [63] W. Alberico, M. Ericson, and A. Molinari, *Ann. Phys. (N.Y.)* **154**, 356 (1984).
- [64] S. Galster, H. Klein, J. Moritz, K. H. Schmidt, D. Wegener, and J. Bleckwenn, *Nucl. Phys. B* **32**, 221 (1971).
- [65] M. J. Dekker, P. J. Brussaard, and J. A. Tjon, *Phys. Rev. C* **49**, 2650 (1994).
- [66] I. Ruiz Simo, J. E. Amaro, M. B. Barbaro, A. De Pace, J. A. Caballero, and T. W. Donnelly, *J. Phys. G* **44**, 065105 (2017).
- [67] I. Ruiz Simo, C. Albertus, J. E. Amaro, M. B. Barbaro, J. A. Caballero, and T. W. Donnelly, *Phys. Rev. D* **90**, 053010 (2014).
- [68] Proteus scientific computing cloud, <https://proteus.ugr.es/en/proteus-eng/>.
- [69] O. Benhar, D. Day, and I. Sick, [arXiv:nucl-ex/0603032](https://arxiv.org/abs/nucl-ex/0603032).
- [70] O. Benhar, D. Day, and I. Sick, <http://faculty.virginia.edu/qes-archive/>.
- [71] O. Benhar, D. Day, and I. Sick, *Rev. Mod. Phys.* **80**, 189 (2008).
- [72] H. C. Kim, S. Schramm, and C. J. Horowitz, *Phys. Rev. C* **53**, 2468 (1996).
- [73] See Supplemental Material at <http://link.aps.org/supplemental/10.1103/PhysRevD.104.113006> for text files with the parameters of Appendices B and C.